Dear Editor,

please find enclosed the new version of the manuscript "Active particles driven by competing spatially dependent self-propulsion and external force" authored by L. Caprini, U. Marini Bettolo Marconi, R. Wittmann and H. Löwen.

We are glad that two of the three reviewers raised very positive judgments on our paper considered suitable for publication in SciPost. Although another referee was more critical, we believe that after our careful revision, accounting for all the suggestions and criticism of the three referees, the new version of the manuscript has improved and sheds more light on the physical relevance of our results to the active matter community.

The text has been amended according to the recommendations of the referees and the relevant changes have been highlighted in red for a faster check. In addition, we made several minor modifications to improve the general readability. In particular, we noticed that the section numbering was missing since on our system, an outdated version of the latex package *titlesec.sty*, which is required by *SciPost.cls*, was installed. We think that pointing out this issue is helpful for authors of future manuscripts.

Below, you can find a point-by-point reply to the reviewers.

Our best regards.

Lorenzo Caprini,
Umberto Marini Bettolo Marconi,
René Wittmann,
Hartmut Löwen.

Reply to Reviewer #1

The authors study an AOUP in a confining harmonic potential with a velocity profile varying periodically in space. It is already known that active particles accumulate where they move slower, this study shows that the competition with an additional confining potential creates unfavourable regions of space - where the restoring force overcomes the propulsion force - such that the density profile transitions from a normal distribution at low persistence length to a multimodal distribution at large persistence. Numerical results are carefully confronted to theoretical expectations

The paper provides, for this simple model, a detailed account of the physics at play in the different regimes of persistence, and should thus serve as a solid basis for follow-up studies on the control of active matter. As such, I recommend publication to SciPost Physics.

We thank the reviewer for the careful reading and for the positive comments on our work.

Below, we report a detailed answer to the reviewer's minor points:

1) **Comment:** *The limits of validity for the unified coloured noise approximation (UCNA) are not detailed in the main text. To which quantities should the persistence time be compared in order to characterise the small/large-persistence regimes? When should*

we expect this approximation to fail?

Reply: We thank the referee for pointing out these important issues. First, the UCNA is valid in general if the matrix $\mathbf{\Lambda}$ is positive definite so that its inverse exists. In the new version of the paper, we elaborate on this point in detail in the third paragraph of Sec. 3.1. *We remark that a necessary condition to obtain predictions (9) and (10) (and, consequently, (11)) is that the matrix* $\mathbf{\Lambda}$ *is positive definite, so that its inverse exists. [...] As a consequence, our approach is supposed to work (at least qualitatively) [...] if (i)* $U(\mathbf{x})$ *is a convex function, (ii)* $U(\mathbf{x})$ *depends on a single Cartesian coordinate or has a positive slope in a radial geometry and (iii) the gradients of* $U(\mathbf{x})$ *and* $u(\mathbf{x})$ *enclose a sufficiently large angle* $\alpha \geq \pi/2$ *[...].* We also mention explicitly the limit of validity in the captions of Figs. 3 and 4.

The persistence time, τ, should be compared in general to the typical time of the dynamics, say the time associated with the presence of the spatial profile of the swim velocity S/v_0 (S = spatial period, v_0 = average swim velocity) and the time induced by the potential, l/v_0 where l is the typical length of the potential that reads $l = k/\gamma v_0$ in the case of a harmonic potential. We expect that the UCNA approximation cannot be more than an approximation working qualitatively when $\tau > S/v_0$ (large persistence regime). In the previous version of the paper, this aspect was described only in the numerical section on the harmonic confinement (above Eq. (18)). In the new version, we discuss the above points in a more general context at an earlier point, in order to clarify the notion of a "small" and "large" persistence time from the beginning. In detail, we write at the end of the first paragraph in Sec. 3.1: *[...] in the small-persistence regime, i.e., when the persistence time is smaller than the other typical times characterizing the dynamics, [...]. In particular, in the present case,* τ *needs to be compared to both the relaxation time due to the potential and to the typical time induced by the spatial modulation of the swim velocity profile (see Sec. 4.1 for an explicit discussion in the specific case of a harmonic oscillator).*

2) **Comment:** *How strong is the approximation of vanishing probability current? What are the consequences of such an approximation?*

Reply: We thank again the referee for this interesting question. By assuming the vanishing of the probability current, we are requiring that the system is locally in equilibrium. This requirement leads to an equilibrium approximation (say, in terms of effective potentials) able to reproduce the non-equilibrium probability distribution. In the small persistence regime (when the persistence time is smaller than the typical time induced by the potential), this approximation works quantitatively, while in the large persistence regime, works qualitatively. We comment on this point in the new version of the paper in the first paragraph in Sec. 3.1: *Our theoretical method employs the vanishing-currents approximation and, as a consequence, allows us to derive an effective equilibrium theory whose validity will be investigated numerically.*

Minor comments:

3) **Comment:** *Above equation (21), is the second derivative of the density profile taken at* $x = 0$*?*

Reply: The referee is right. We fix this issue by adding *at* $x = 0$ in the new version of the manuscript.

4) **Comment:** *On top of page 12, (3) is not a prediction, should it rather be (9)?*

Reply: We are grateful to the referee for his/her careful reading and corrected this typo.

5) **Comment:** *In Fig. 4, could you add density profiles so that comparisons can be made similarly to all other figures?*
Reply: Following the suggestion of the referee, the density profiles have been included in Fig. 4 in the new version of the paper.

Reply to Reviewer #2

This paper studies an active particle (AOUP) with spatially-dependent activity in a confining potential and more especially in a harmonic well. The authors have a written english of good quality which makes the reading pleasant. In the first half of the paper, they tackle their model analytically by using two approaches: the UCNA approximation and an exact perturbative scheme. While I did not try to reproduce their computations in details, their study seems rigorous and well-grounded in the literature: the uncontrolled assumptions are stated and the terms neglected are mentioned. In the second half of the paper, the authors perform numerical work to support their study. They distinguish three regimes for the density depending on the parameter $v_0\tau/S$: monomodality, bimodality and multimodality. For each of these three regimes, they also supply the distribution of the velocity as well as its variance when the spatial position is varied. Despite all these results, I had troubles to understand the novelty or the take-home message of the paper. In particular, I have four major concerns which I develop below

We thank the reviewer for his/her careful reading of the paper and for all the interesting questions and doubts, which helped us a lot to spot and improve and strengthen the message of our paper. However, despite the referee's global judgment on our paper, we believe that studying the interplay between a space-dependent swim velocity and an external potential represents an interesting step for active matter systems which could be helpful for applications. In particular, we coined the following take-home message, stated in the last two sentences of the conclusions: *We demonstrated that by combining these two physically distinct effects, it is possible to generate complex density patterns through two relatively simple fields, which is surely easier to realize in practice than generating a single external field with a complex shape. This possibility to fine-tune the stationary properties of active particles in experimental systems opens up a new avenue for future applications and developments.* Moreover, we added the following statement to the abstract: *We thus demonstrate that the interplay of two relatively simple physical fields can be utilized to generate complex emerging behavior.*

Here, we reply to the main issues raised by the referee:

1) **Comment:** *To which extent is taking a spatially-dependent self-propulsion u(x, t) different than just having a single AOUP in a complicated potential? From the authors results, it does not seem that there is unexpected physics due to the spatially-dependent u(x, t). In particular, all the features highlighted by the authors for an AOUP with spatially-dependent self- propulsion (accumulation near walls for example) are already present for an AOUP with constant self-propulsion. I have remarked that, when u(x) is a bijection, one can map the dynamics (3) of the authors to the dynamics of an AOUP with spatially-independent self-propulsion by making the change*

of variable $\tilde{u} = ln(u(x))$. Indeed, dividing both sides of (3) by $u(x)$ leads to

$$\frac{\dot{x}}{u} = -\frac{\nabla U}{u} + \eta\,, \qquad \rightarrow \dot{\tilde{u}} = g(\tilde{u}) + \eta \tag{1}$$

where $g(\tilde{u}) = \nabla U(u^{-1}(e^{\tilde{u}}))/e^{\tilde{u}}$ and η is an Orstein-Uhlenbeck process as described in (2b) of the paper.

Reply: We thank the referee for raising such a point, which indicates that the different steps in our approximation scheme, which necessarily lead to a nontrivial coupling between self propulsion and potential, have not been properly motivated. In particular, rewriting the dynamics in a form that involves $\dot{x}/u$, as suggested in the referee's equation (1), is a crucial step to deal with the multiplicative nature of the noise which results in our model from the spatial modulation of the swim velocity. However, the suggested transformation (1) is not correct, as we outline in the following.

Indeed, if we define a new variable

$$\tilde{u} = \ln u(x) \quad \Leftrightarrow \quad u(x) = e^{\tilde{u}}$$

As suggested by the referee, we get:

$$\frac{d\tilde{u}}{dt} = \frac{d\tilde{u}}{du}\frac{du}{dx}\frac{dx}{dt} = \frac{u'(x)}{u(x)}\dot{x} = \frac{u'(x)}{u(x)}\Big(-\nabla U(x) + u(x)\eta\Big) = u'(x)(-g(\tilde{u}) + \eta)$$

This expression contains an extra factor $u'(x)$ with respect to Eq. (1) written by the referee (and also a minus sign in front of $g(\tilde{u})$ that is clearly a typo). This factor is, however, particularly relevant because the new system (the one described by $\tilde{u}$) still has a multiplicative noise and thus requires further theoretical treatment. Moreover, the coupling between the gradients of both fields is already evident. As a consequence, the original active system with a spatial dependent swim velocity cannot be easily mapped onto a system with spatially-independent self-propulsion.

What the referee may have meant to show is practically exactly the idea behind UCNA: one must both eliminate the multiplicative nature of the noise and replace the colored noise by a white noise through a change of variables. Due to the latter substitution, the necessary coupling between gradients of $u(x)$ and $U(x)$ and thus the invalidity of a simple mapping becomes apparent. We added two comments in the manuscript, further elaborating on which theoretical steps are necessary, which might help to avoid such misconceptions. At the beginning of Sec. 2.2 we write *Our equation of motion (2a) of an AOUP with a spatially dependent swim velocity contains a multiplicative colored noise, which does not readily allow us to gain further analytic insight. As a first step [...].* Then, in the first paragraph of Sec. 3.1, we sum up the crucial steps of our approximation scheme as follows: *having derived the auxiliary dynamics (6), where the colored noise $\boldsymbol{\eta}$ is replaced by a white noise $\boldsymbol{\chi}$, we formally identify a new variable $\dot{\mathbf{z}} := \dot{\mathbf{x}}/u(\mathbf{x})$ to eliminate the multiplicative nature of the noise and then neglect the generalized inertial term $\propto \ddot{\mathbf{z}}$ in Eq. (6b).*

Now, we provide an answer to the central concern of the referee:

From (1), I intuitively do not expect much differences between an AOUP with a spatially-dependent self-propulsion and one with a constant self-propulsion in a more complicated potential. Have the authors studied the question?'

We thank the referee for raising such a point that we think is particularly interesting. Of course, it is possible to obtain a certain "target" density profile in different ways, but the underlying physics are crucially different. Therefore, a system with a spatially-dependent self-propulsion cannot be mapped onto a system with a complicated potential. This can be understood in two ways.

The first argument is a mathematical one. As laid out above, it is not possible to map the coupled gradients of the two fields onto a single effective field. To emphasize this point, we stress in our revised manuscript on several occasions that the interplay of both fields results in new physics, for example in the last sentence of Sec. 2.2 or by stating in the conclusion that *the deviations of the velocity distributions from a Gaussian shape exclusively arise from the interplay of these two fields.*

The second argument comes from a consideration of the underlying physics, which we lay out in the final paragraph of Sec. 2.2: *Indeed, $u(\mathbf{x})$ provides an additional contribution to the effective friction in the dynamics of $\mathbf{v}$ but does not give any contributions to the confining force, at variance with the potential $U(\mathbf{x})$ that affects both the force acting on the particle and the effective friction matrix.* Moreover, we discuss an explicit counter-example in footnote [76], which reads: *To shed light on the essential physical difference between a confined particle with uniform swim velocity and a free particle subject to a swim-velocity profile, let us consider, as a basic example, an AOUP with constant swim velocity $u(x) = v_0$ trapped in a harmonic potential, system (i), whose exact stationary density profile $\rho(x)$ has a Gaussian shape. In principle, this distribution can also be realized in the absence of external forces by a swim-velocity profile of the form $u(x) \propto 1/\rho(x)$, system (ii), but the physics are crucially distinct. In case (i), the particle is confined and can explore the region far from the minimum of the potential only because of fluctuations induced by the active force. The Gaussian density profile in system (ii) is obtained because the particle spends more time in the central region where it moves slowly. However, due to the absence of external forces (or other confining mechanisms), the diverging swim velocity allows the particle to escape to infinity. This means that such an effective confinement can only formally be achieved through periodic boundary conditions: the particle moves slowly in the minimum of $u(x)$, escapes rightwards (or leftwards) with an increasing swim velocity and approaches again the slow region by coming back from the other side of the box.*

2) **Comment:** *The authors results can be obtained by applying two main results of active matter that are already well-established. The first one is that active particle with spatially-dependent self-propulsion $u(x)$ accumulate where they are slow as $\rho(x) \sim 1/u(x)$ (Refs [28] and [29] in the introduction). The second one is that confining an active particle with a potential U leads to an accumulation at the position where the force $\nabla U(x)$ is equal to the self- propulsion amplitude u (Ref [71] and [86] from the authors). This last result, which has been documented, could also be seen as a consequence of the former one: the confining force effectively reduces the self-propulsion of the active particle which in turn triggers an accumulation due to slowness. Figure 1 and figure 2 are intuitively explained in light of these two established results. For example, in figure 1d, spikes of the density correspond to positions where $\nabla U(x) = u(x)$. In figure 2d, the two spikes close to the center correspond to local minima of $u(x)$ while the two highest peaks correspond to both local minima of $u(x)$ and positions where $\nabla U(x) = u(x)$. Thus, it is not surprising that these spikes are the highest ones: the effective self-propulsion at these positions is lowered*

by the potential compared to the self-propulsion at the center. Finally, I believe that the bimodality of the velocity distribution displayed in figure 3h is not surprising; it is due to particles coming from the cluster on the right and going leftway as well as to particles coming from the cluster on the left and going rightway. Because the confining force increases away from the center, the position of the spike with negative velocity diminushes from yellow to brown while the trend is opposite for the spike with positive velocity.

Reply: (Refs. [71] and [86] are now Refs. [75] and [91].) We thank the referee for his/her interesting remarks. We agree on the explanations of Figs. 1 and 2, given by the referee that is contained also in our manuscript. However, we think that the results in the simultaneous presence of a confining force and a swim velocity profile is less intuitive than the case $u(x) = v_0$ and needs to be carefully explained and demonstrated. In addition, despite the qualitative picture explained by the referee (and by us in the paper) gives an explanation, is still remarkable that our theoretical approach is able to reproduce (quantitatively in the small persistence regime) and qualitatively (in the large persistence regime), the results of the simulations. In particular, we thank the referee for his/her remark about the velocity distribution, which provides a nice intuitive picture to interpret and reinforce the results that we have obtained. Therefore, we included a few remarks accounting for the above comment of the referee in the new version of the manuscript to increase the physical understanding of Fig. 3. The discussion is appended at the end of Sec. 4.3.

In short, we do not believe that our predicted behavior is generally obvious, in particular to the less experienced reader, who will surely appreciate the effort of providing both a detailed numerical and theoretical study on the interplay of different driving forces and an intuitive explanation in terms of force balance arguments. This is particularly the case in the light of the different physics underlying external confinement and spatially varying self propulsion, which we already elaborated on after the previous comment.

3) **Comment:** *I do not see what is the new physics brought forward in this work which has not already been discussed in Ref [70] by the authors. For example, in the present paper, the authors affirm that the interplay between the external force and the modulation of the swim velocity can be used to manipulate the behavior of a confined active particle, for instance by locally increasing the kinetic temperature or by forcing the particles to accumulate in distinct spatial regions with different probability. However, in their previous work [70], the authors have already demonstrated that the density of their model follows the law $\rho(x) \sim 1/u(x)$ in the absence of potential. Thus there is no need of a confining potential if one wants to sort and accumulate active particles in distinct regions: a spatially- dependent self-propulsion is enough.*

Reply: (Ref. [70] is now Ref. [74].) A system of active particles with a spatially modulated swim velocity (as the sinusoidal-like one used in the experiments in Ref. [19] C. Lozano et al., Nat. Comm. **7**, 12828 (2016)) can be used to favor some regions of space, because of the law $\rho(x) \sim 1/u(x)$. Moreover, the system shows a diffusive-like behavior, as shown in Ref. [74]: after a typical time, the active particle leaves the region with small $u(x)$ (say a minimum of the sinusoidal function) to escape away (approaching another minimum of $u(x)$ in the case of the sinusoidal profile). Thus, a simple profile $u(x)$ cannot be employed to confine active particles (recall the physical argument, laid out in response to the first comment and presented at the end of Sec. 2.2 in the new version of the manuscript).

What is the motivation and the new physics when studying the interplay between a potential and a spatially-dependent self-propulsion?

Reply: As laid out before, there is not a simple mapping to an effective external potential, so new physics naturally arise. We have shown that the interplay between an external force and a spatially modulating swim velocity can be used to manipulate the behavior of a confined active particle, for instance by locally increasing the kinetic temperature or by forcing the particles to accumulate in particular spatial regions with different probability. One example for new physics becomes apparent when regarding the velocity profile. In both cases of considering only a harmonic trap or only a spatially dependent velocity profile, the velocity distribution is Gaussian. However, we observed emerging non-Gaussian behavior when combining these two fields. To emphasize this we speak in Sec. 4.3 of a *non-Gaussianity induced by the interplay of confinement and spatially modulating swim velocity.*

One central motivation of our study comes from the experimental realizability of complex density patterns. Given the discussion above, to favor some regions of space but still confining the system, we studied the interplay between a spatial-dependent swim velocity (which can be easily obtained with active colloids or active bacteria) and an external harmonic potential (harmonic traps have been obtained both in case of bacteria and colloids while realizing more complex potentials could be less easy from an experimental perspective). This complex interplay of two simple fields is surely easier to impose than a single external field with high fluctuations. As mentioned above, this is now concluded in the final paragraph of the conclusions and also in the final sentence of the abstract.

4) **Comment:** *As the authors point out in their work [70], there is already a literature studying spatially- dependent self-propulsion amplitude and memory time for AOUP (ref [61] for example). In [70], the authors detailed, from a mathematical point of view, why their model (2) is actually different from the model studied in [61]. However, from a physical point of view, the difference remains unclear: what are the physical features present in (2) that are not in [61]? In particular, when it comes to experiments [25-27], what is the correct model one should use? It would be interesting if the authors show that their model is indeed the one relevant for the experiments.*

Reply: (Refs. [61] and [70] are now Refs. [63] and [74].) We thank the referee for this interesting question which requires a discussion. The main difference between our model and the model of Ref. [63] [i.e., the former Ref. [61] D. Martin et al., Phys. Rev. E **103**(3), 032607 (2021)] concerns the validity of the law:

$$\rho(x) \sim 1/u(x)\,. \tag{2}$$

In the model of Ref. [63] without external forces, Eq. (2) can be obtained only perturbatively when $u(x)$ changes "slowly" (with respect to the persistence length), while this law is violated if $u(x)$ changes "rapidly". In our model, in the absence of external force, Eq. (2) holds independently of the parameter choice. As a consequence, our model seems to be more suitable to describe the experimental active systems such that Eq. (2) holds: for instance, the active colloids studied by the group of Bechinger [see for instance Ref. [19] Lozano et al., Nat. Comm. **7**, 12828 (2016)] and the bacteria studied by the group of Di Leonardo [see for instance Ref. [27] G. Frangipane et al., Elife **7**, e36608 (2018)] or by the group of Poon [see for instance Ref. [25] J. Arlt et al., Nat. Comm. **9**, 768 (2018).]

In the new version of the manuscript, we discuss in the final paragraph of Sec. 2.1 that *the spatial dependence of the self propulsion velocity can be conveniently accounted for through a multiplicative factor $u(\mathbf{x}, t)$, which does not affect the dynamics of the noise vector* and that *our AOUP model is more suitable to describe the class of experimental systems for which the relation $\rho(\mathbf{x}) \sim 1/u(\mathbf{x})$ is observed [...]. We expect that this consistency is also an advantage for describing interacting systems.*

Below, we answer the minor points raised by the reviewer:

1) **Comment:** *I did not see an indication about the dimension considered in simulations: are there performed in $d = 1$ or $d = 2$?*
Reply: Simulations are realized in one dimension. The referee is right that this might have been easy to overlook since our intention was to demonstrate an approximation holding for more general systems, before specifying that we focus on the one-dimensional case in the numerical section 4. To this end, we added a subsection heading 4.1 *Swim-velocity profile and external potential in one dimension.* To further emphasize this point, we added an additional remark on the dimensions of the system after Eq. (17), which reads *This choice and the features of the AOUP allow us to consider directly a one- dimensional system, essentially focusing only on the x component and neglecting the dynamics of the other spatial coordinates.* Moreover, we now state in the caption of all figures that *Simulations are realized in one spatial dimension.*

2) **Comment:** *the change of variable presented right after (3) might benefit from a clearer presentation. I was first confused about whether v included the confining force.*
Reply: We thank the referee for this suggestion. Yes, the velocity $\mathbf{v}$ does include the confining force. In the new version of the manuscript, we added the following explanation: *To derive the dynamics in the variables $\mathbf{x}$ and $\mathbf{v}$, we adopt a simple strategy whose leading steps are reported in details in Appendix A. We perform the time-derivative of Eq. (3), substitute $\dot{\boldsymbol{\eta}}$ with Eq. (2b) and then replace $\boldsymbol{\eta}$ with $\mathbf{v}$ and $U(\mathbf{x})$, using again Eq. (3), and finally obtain an equivalent equation of motion for the velocity $\mathbf{v}$.*

3) **Comment:** *In the appendix eq (27), one side has $u(x)$ while the other has $u(x, t)$*
Reply: We thank the referee for the careful reading. We have fixed this typo in the new version of the paper.

4) **Comment:** *Right before the part on density distribution: when $v_0\tau/S$ grows, the spatial period of $u(x)$ increases should be when $v_0\tau/S$ grows, the spatial period of $u(x)$ decreases if I understood correctly the authors (S being the spatial period).*
Reply: We thank the referee for the careful reading. We correct this mistake in the new version of the paper.

5) **Comment:** *Right in the beginning of the part Velocity distribution, display an almost Gaussian shape in agreement with Eq (3) should probably be display an almost Gaussian shape in agreement with Eq (10). The same reference lapsus is also found later in the same part Gaussian distribution with space-dependent variance given by Eq (3).*
Reply: We thank again the referee: these typos have been fixed.

6) **Comment:** *On figure 3; is the x-axis rescaled? Is it x or $\tilde{x}$?*
Reply: we are grateful that the referee noticed this inconsistency and added the label $x/(v_0\tau)$ to the horizontal axes. Moreover, to avoid further confusion in the bottom plots, we also specify $x = \bar{x}v_0\tau$ in the caption.

7) **Comment:** *In the end of the part called profile of the kinetic temperature, I could not understand well the phrase the variance of the particle velocity becomes steeper and decreases to zero in the regions which are not explored by the particle. This is consistent with the scenario observed in Fig. 1 (c): the particles accumulate in the regions where they move slowly and the velocity variance is small. How can particles accumulate in regions that they do not explore?*
Reply: We thank the referee for his/her careful reading and, in particular, to evidence such an unclear sentence which has been rephrased as follows: *When $v_0\tau/S$ increases, e.g., due to a shorter periodicity S of the swim-velocity $u(x)$, $\langle v^2(x)\rangle$ decreases upon moving away from the potential minimum.* For further clarity of the comparison, we added the corresponding density profiles to Fig. 4 and then continue with *This is consistent with the scenario observed in Fig. 4 (a).*

Reply to Reviewer #3

We thank the reviewer for his/her careful reading and positive judgment on our work, summarized in the following sentence:
I found the subject of the lecture note interesting and the problem they focused on looks timely.

Here, we reply to the main issue raised by the referee:

1) **Comment:** *It is not completely clear to me how the velocity of the particle is controlled in this model. In the sense that η fluctuates with a variance that is proportional to $1/\tau$ and then the velocity is basically $u(x,t)\eta$. For $u(x,t) = v_0$, it looks to me that velocity is not really controlled unless you change the variance of the OU process. I might be wrong, however, I think that a general reader might be getting wrong like me and thus I would suggest the authors clarify this point.*
Reply: We thank the referee for raising this point. The process $\boldsymbol{\eta}$ evolves as

$$\dot{\boldsymbol{\eta}} = -\frac{\boldsymbol{\eta}}{\tau} + \frac{\sqrt{2}}{\sqrt{\tau}}\boldsymbol{\chi} \tag{3}$$

which corresponds to Eq. (2b) except from a global τ factor multiplied at both sides. As a consequence, the process $\boldsymbol{\eta}$ has unit variance in one spatial dimension and the corresponding reduced probability distribution

$$p(\boldsymbol{\eta}) \sim e^{-\frac{\boldsymbol{\eta}^2}{2}} \tag{4}$$

does not depend on τ. For this reason, the swim velocity (the variance for instance) does not change if we increase τ.

To remove this possible source of confusion, we stress on several occasions in the new version of the manuscript that $\boldsymbol{\eta}$ has unit variance, most notably directly after Eq. (1)

and clarify in the completely revised final paragraph of Sec. 2.1 that *the Ornstein-Uhlenbeck process in Eq. (2b) has unit equal-time variance (except for a dimensional factor which we ignore here for convenience [73]), such that the reduced stationary probability distribution of* $\boldsymbol{\eta}$ *does not depend on the time scale* τ*. This means that* $u(\mathbf{x})$ *provides a unique velocity scale. Moreover, this unit-variance version of the AOUP model allows us to establish a direct link to the ABP model...*

2) **Comment:** *I did not find clear the presentation in the section Velocity description of AOUP. It seems to me that they just perform the time derivative of Eq. (3) and then they consider the usual UCN approximation* ($\tau x = 0$)*. I do not think an appendix of just two lines is required (see eq. (22) and (23)) since this derivation might be very useful for the general reader. Moreover, they introduce the Jacobian but a) they do not write its expression, and b) Does occur any problem if* $J = 0$*? I am asking that because after (1) they require* $u \geq 0$*, however,* $|J| = u$ *and the approximated solution seems to require* $u > 0$*. Is this a problem of the approximation or, more in general, the model is not defined for* $u = 0$*?*

Reply: In the Section "velocity description of AOUP", we perform a change of variable, by switching from $(\mathbf{x}, \mathbf{f}^a) \to (\mathbf{x}, \mathbf{v})$. This theoretical step is fundamental to deriving the UCNA distribution both in position and velocity domains. This operation can be achieved by deriving the equation of motion for $\mathbf{x}$ with respect to time and by replacing $\dot{\mathbf{f}}^a$ and successively $\mathbf{f}^a$ with functions of $\mathbf{x}$ and $\mathbf{v}$ provided by the equation of motion itself. These algebraic passages have been detailed in the appendix to help a reader to perform calculations. The referee is right that this is an important section and we have carefully revised it, for example by explaining in more detail before Eq. (6) how it is derived. Regarding the two points of the referee, in particular, we made the following modifications:

a) In the main text, we report the expression for the Jacobian of the transformation (i.e., the determinant $\det[\mathcal{J}]$ of the Jacobian matrix $\mathcal{J}$), which is reported in Eq. (4). For clarity, we added the full expression of $\mathcal{J}$, namely,

$$\mathcal{J} = \frac{\partial \mathbf{b}}{\partial \mathbf{a}} = \begin{bmatrix} \frac{\partial \mathbf{x}'}{\partial \mathbf{x}} & \frac{\partial \mathbf{x}'}{\partial \boldsymbol{\eta}} \\ \frac{\partial \mathbf{v}}{\partial \mathbf{x}} & \frac{\partial \mathbf{v}}{\partial \boldsymbol{\eta}} \end{bmatrix} = \begin{bmatrix} 1 & 0 \\ 0 & u(\mathbf{x}) \end{bmatrix}$$

and further explanations to Appendix A.

b) We thank the referee for raising such a point. The referee is completely right. The transformation cannot be achieved for $u = 0$ which is rather non-physical because we can neglect the thermal noise due to the solvent only if $D_a = u^2\tau \gg D_t$, a condition which cannot be satisfied if $u = 0$. In practice, when $u = 0$ the system evolves deterministically (without noise) and this is also a source of technical problems. We thus clarify after Eq. (5) *that the condition* $u(\mathbf{x}, t) > 0$ *implies* $det[\mathcal{J}] > 0$ *and, thus guarantees the possibility of performing the transformation.*

3) **Comment:** *I think Eq. (7) requires some warnings because, in the region where the potential develops negative curvatures, one ends with negative friction. I understand the authors choose a safe potential with always positive curvature (basically this is also the reason why for large* τ *one can obtain a good approximation of stationary configurations). For instance, it looks to me that even in a small* τ *limit negative and large curvatures might cause problems. (a) Could the authors comment on that and also include relevant references? (b) I think a similar discussion is required once they introduce* $\Lambda(x)$

Reply: We thank the referee for this question. In the small-τ regime, the matrices $\mathbf{\Gamma}(\mathbf{x})$ and $\mathbf{\Lambda}(\mathbf{x})$ are always positive, because they are of the form $\mathbf{I}+\tau\mathbf{f}(\mathbf{x})$, where $\mathbf{I}$ is the identity matrix and $\mathbf{f}(\mathbf{x})$ is a vectorial function of $\mathbf{x}$ which contains all the terms in Eq. (7) and Eq. (8). As a consequence, there exists always a value of τ (small enough compared to the other relevant time scales) below which the matrices remain positive. We also stress that the dynamics (6) is also defined for negative $\mathbf{\Lambda}(\mathbf{x})$ (or $\mathbf{\Gamma}(\mathbf{x})$), while the restrictions provided above come into play to derive the approximations given by Eq. (9) and Eq. (10). For this reason, we state at the beginning of Sec. 2 that *So far, all steps in Sec. 2.2 were exact and the drawn conclusions general.* A detailed discussion of the aforementioned shortcomings of the approximations has been added as the third paragraph of Sec. 3.1.

4) **Comment:** *In section Theoretical Predictions should contain all the relevant information about the approximations made to arrive at Eqs. (9) and (10) are valid. Moreover, in Eq. (10), obtained within UCN, there is a det $\Lambda(x)$ that does not appear in Fox: this is because Fox is a small τ approximation (the authors write The same $\rho(x)$ can be obtained the path-integral method proposed by Fox). I understand the small τ of UCN brings to Fox, however, in UCN one just asks for large friction. (a) Could the authors clarify this point? Also, (10) has clearly a problem with negative values of Λ but also with $u = 0$, (b) could the authors provide a list of conditions under which the approximated solution is valid? (c) Again, I think there are conditions for writing Eq. (9). In appendix (B) they show how to obtain $\rho(x)$ but I did not find information in Eq. (9).*
Reply: The referee is right that no assumption about the large-τ behavior enters the derivation of the Fox approximation. As such, UCNA and Fox are two different approximation schemes that also predict different dynamics. However, both lead to the same steady-state probability distribution in the absence of translational diffusion coefficient, say $D_t = 0$. Different steady-state results in the two cases occur only if $D_t > 0$ (see for instance Ref. [72] R. Wittmann et al., Journal of Statistical Mechanics: Theory and Experiment, 2017). To clarify this, we extend the mentioned statement to *In the absence of thermal noise, the same (stationary) $\rho(\mathbf{x})$ can be obtained using the path-integral method proposed by Fox* and also added further theoretical details to the first paragraph of Sec. 3.1.

As stated above and elaborated in the new version of the manuscript (third paragraph of Sec. 3.1), Eq. (9) and Eq. (10) hold globally if $\mathbf{\Lambda}(\mathbf{x})$ is positive, which can be achieved for every τ only under certain conditions. More details regarding the derivation of Eq. (9) have been included. We also specified that (26) is an *approximate condition*, where we also cite [82] for further reference.

5) **Comment:** *The theory has been checked against numerical simulations in one spatial dimension. Does the approximated solution presented in (10) hold also in two dimensions? I think the authors should clarify the reasons why they focus their attention on one-dimensional problems.*
Reply: The theory (i.e., Eqs. (9) and (10)) hold for general dimensions. In the numerical study, we focused on a one-dimensional system because we have chosen a one-dimensional profile for $u(\mathbf{x})$ taking inspiration from experiments (see Ref. [19] C. Lozano et al., Nat. Comm. **7**, 12828 (2016)). Indeed, the new physics is only contained along the spatial direction where the swim velocity profile presents changes.

The aspect of dimensionality is also taken into account in our new discussion on

the validity of the theoretical approximations in the third paragraph of Sec. 3.1, see above. Moreover, we added the following remark to the third paragraph of the conclusion: *Despite our particular attention to one spatial dimension, we recall that we practically obtain the same results for a planar geometry in higher spatial dimensions and that we expect that our theory is also suitable for sufficiently well-behaved potentials and velocity fields in other geometries (compare the discussion in Sec. 3.1).*

6) **Comment:** *In the section The harmonic oscillator they write we have shown that our analytical predictions from Eqs. (9), (10) and (11) are exact in the small persistence regime through analytical arguments. I do not see where a small tau approximation enters (10).*
Reply:

The assumption of small τ does not enter directly in the derivation of Eqs. (9), (10) and (11). However, one of the key passages of the derivation is fully justified only if τ is small, in particular, when we get the overdamped dynamics Eq. (30) (Appendix B) by neglecting the acceleration term (Eq. (29)). To emphasize this point, we now state *Assuming that the velocity relaxes faster than the position (as for example in the small-persistence regime) allows us to neglect both these terms.*

In addition, we have reported the exact expression for the probability distribution $p(x, v)$ perturbartively as a function of τ (In Eq. (14)). The first order in τ of $p(x, v)$ coincides with the UCNA solution. Thus, for small τ our approximation is exact Starting from the order τ^2 additional terms arise in the perturbative expression for $p(x, v)$. As a consequence, our Eqs. (9), (10) and (11) are not exact but only provide a useful approximation. To be clearer, we replaced the reference to Sec. 3 by Sec. 3.2 in the statement quoted by the referee.

7) **Comment:** *I think it might be very useful to the reader if the authors could add more details about the comparison between numerical results with Eq. (10).*

(a) Could the authors write the expression they use in 1 dim?

(b) Could the authors say how the comparison has been performed, i.e., they integrate numerically eq. (9)?
Reply: We thank the referee for these questions, which help to put more clarity in our presentation. In our revised manuscript, we refer to the following points explicitly in Sec. 4 and in the captions of the corresponding figures:

a) The theoretical expressions used in 1d are provided by Eq. (16) [which is the one-dimensional expression for the steady-state spatial density profile, Eq. (10)] and the one-dimensional version of Eq. (9) [i.e., the predictions for $p(x, v)$ containing the explicit dependence on $\mathbf{v}$, which is nothing but a Gaussian in v], where $\Lambda(x)$ is given by Eq. (19).

b) The integral occurring in the analytical expression for $\rho_s(x)$ in Eq. (9) has been performed numerically (using Mathematica) because the explicit expression for the integral is unknown for our choice of $U(x)$ and $u(x)$.

8) **Comment:** *In Conclusions they write we have developed a theoretical treatment, applicable to rather general choices of confining potentials and inhomogeneous swim velocities. I think the sentence should be updated once they answer to (4).*
Reply: To account for the modifications described above, we removed the part

applicable to rather general choices of confining potentials and inhomogeneous swim velocities of the aforementioned sentence and, instead write in the third paragraph of the conclusion: *Despite our particular attention to one spatial dimension, we recall that we practically obtain the same results for a planar geometry in higher spatial dimensions and that we expect that our theory is also suitable for sufficiently well-behaved potentials and velocity fields in other geometries (compare the discussion in Sec. 3.1).*

Below, we answer the minor points raised by the reviewer:

1) **Comment:** *In the main text the authors indicate different appendix with capital letters, however, there are no letters in the appendix section.*
Reply: We thank the referee for his/her careful reading and pointing out this technical problem, which has now been resolved by using an updated package.

2) **Comment:** *Introduction: The motility of active particles is much higher than that of their passive counterparts What does it mean? A passive bead immersed in a thermal bath is not motile. I think the authors mean that motility induces a diffusive regime whose diffusion constant is much bigger than that due to the thermal bath. I would ask the authors to state properly this sentence.*
Reply: We are grateful to the referee for pointing out such a mistake, which is corrected in the new version of the paper by speaking of a diffusivity instead.

3) **Comment:** *Abstract: Our results can be confirmed by real-space experiments on active colloidal Janus particles in the external field. Usually, Janus particles are well captured by Active Brownian motion rather than AOUP,*
Reply: The referee is right, we removed this sentence from the abstract and replaced it with the more general and even more important conclusion that *We thus demonstrate that the interplay of two relatively simple physical fields can be utilized to generate complex emerging behavior.*

4) **Comment:** *Introduction: The ABP model is harder to use to make theoretical progress it does not look totally true to me, there are several theoretical works where the coarse-graining properties of active systems are obtained from ABP (see for instance T Speck, AM Menzel, J Bialké, H Löwen The Journal of chemical physics 142 (22), 224109) and RT (ME Cates, J Tailleur Annu. Rev. Condens. Matter Phys. 6 (1), 219-244) or even starting from minimal swimmer models (A Baskaran, MC Marchetti Proceedings of the National Academy of Sciences 106 (37), 15567-15572).*

Reply: Our intention was only to say that, according to our experience in the field, theoretical predictions can be obtained quite easily in the case of the AOUP model with respect to the ABP model. Anyway, the referee is right and, of course, there are some theoretical contributions obtained through the ABP model (without employing the AOUP approximation). Thus, we follow his/her suggestion and we reduce our claim, by rephrasing that sentence and citing the references suggested by the referee.

5) **Comment:** *Introduction: AOUP model is recovered upon substituting $v_0^2 = D_a/\tau$ I think in d dimensions (that is the situation where they are working in 2a and 2b, otherwise bold symbols do not make any sense) $D_a = v_0^2\tau/d$.*
Reply: We thank the reviewer for pointing out this issue, which tells us that we have not been clear enough on our notational convention. In our manuscript, we

simply choose to work with $D_a = v_0^2\tau$ for convenience of our notation (avoiding the dimensional factor d). We are aware of the usual mapping and discuss it in the footnote [69] (old version) and now [73], which is reported here for clarity: *The common mapping between ABPs and AOUPs in $d > 1$ spatial dimensions relates the persistence time $\tau = D_r^{-1}/(d-1)$ and the active diffusion coefficient $D_a = v_0^2\tau/d$ of the AOUP model to the rotational diffusivity D_r and self-propulsion-velocity scale v_0 of the ABP model [72]. To ease the notation for the predictions of our generalized AOUP model, we follow the convention of Ref.[74] and do not imply this mapping, simply setting $d = 1$, which gives the same physics. If one wishes to make explicit contact to the ABP model for $d > 1$, the last term in Eq. (2b) should be replaced by $\sqrt{2\tau/d}\boldsymbol{\chi}$, such that the formulas subsequently derived for arbitrary spatial dimension d should be interpreted by rescaling $u(\mathbf{x}) \to u(\mathbf{x})/\sqrt{d}$.*

In the new version of manuscript, we completely reworded the paragraph of the main text discussing these points to make it clearer that all details are given in [73], emphasizing that this is a footnote and not a reference. The relevant comments read: *(except for a dimensional factor which we ignore here for convenience [73])* and $D_a = v_0^2\tau$ *(see also footnote [73] for a general discussion of the mapping between ABPs and the different versions of AOUPs in d spatial dimensions).*

6) **Comment:** *In section Model I think they start with considering AOUP in two spatial dimensions (since they write η is a two-dimensional Ornstein-Uhlenbeck process) however, I believe this information might get missed by a distracted reader. Could the authors introduce at the beginning of the section if they work in 1,2 or d spatial dimensions?*
Reply: We thank the referee for pointing out this inconsistency. In the first sections, our intention was to show an approximation holding for more general systems than the one-dimensional one discussed in the numerical section (say, holding for general dimensions and general swim velocity profiles). For this reason, we did not intend to specify the spatial dimensions until the numerical part in Sec. 4. Therefore, we removed the specification "two-dimensional" after equation (1).

7) **Comment:** *Figure 1: why the linear force looks like $|x|$?*
Reply: We thank the referee for the careful reading. When the particle is stuck into an accumulation region such that $x < 0$, the active force is negative, say $\eta < 0$. On the contrary, if the particle is stuck at $x > 0$ the active force is positive, say $\eta > 0$. This occurs because for $x < 0$, the linear force due to the potential pushes the particle to $x = 0$ so that $F(x) > 0$ while for $x > 0$ we have $F(x) < 0$. As a consequence, the modulus of the active force, say $\mathbf{u}(x)$, needs to be compared with the modulus of the potential force, $|F(x)|$.

Speaking of a linear force instead of the modulus of a linear force was a typo, which we corrected in the caption of Fig. 1 and Fig. 2 and in the text.

Active particles driven by competing spatially dependent self-propulsion and external force

Lorenzo Caprini[1⋆], Umberto Marini Bettolo Marconi[2] and René Wittmann[1], Hartmut Löwen[1]

1 Heinrich-Heine-Universität Düsseldorf, Institut für Theoretische Physik II - Soft Matter, D-40225 Düsseldorf, Germany
2 Scuola di Scienze e Tecnologie, Università di Camerino, Via Madonna delle Carceri, I-62032, Camerino, Italy
⋆ lorenzo.caprini@hhu.de, lorenzo.caprini@gssi.it

June 7, 2022

Abstract

We investigate how the competing presence of a nonuniform motility landscape and an external confining field affects the properties of active particles. We employ the active Ornstein-Uhlenbeck particle (AOUP) model with a periodic swim-velocity profile to derive analytical approximations for the steady-state probability distribution of position and velocity, encompassing both the Unified Colored Noise Approximation and the theory of potential-free active particles with spatially dependent swim velocity recently developed. We test the theory by confining an active particle in a harmonic trap, which gives rise to interesting properties, such as a transition from a unimodal to a bimodal (and, eventually multimodal) spatial density, induced by decreasing the spatial period of the self propulsion. Correspondingly, the velocity distribution shows pronounced deviations from the Gaussian shape, even displaying a bimodal profile in the high-motility regions. We thus show that the interplay of two relatively simple physical fields can be employed to generate complex emerging behavior.

Contents

1 Introduction

The control of active matter [1–4] is an important issue for technological, biological and medical applications and has recently stimulated many experimental and theoretical works. It is also very important in the future perspective of self-assembling and nano-fabricating active materials. The diffusivity of active particles is much higher than the one of their passive counterparts. Indeed, the former may be caused by high motility induced by either an internal "motor" (metabolic processes, chemical reactions, etc.) or a directed external driving force acting on each particle, while the latter is simply due to random collisions with the particles of the thermal bath. This property offers intriguing perspectives since it is possible to achieve navigation control of active particles [5,6], for instance when driving their trajectories by some feedback mechanism [7,8].

In the case of active colloids, such as Janus particles activated by external stimuli, the motility can be tuned by modulating the intensity of light [9–14]. This property has been employed to trap them [15,16] and to obtain polarization patterns induced by motility gradients [17,18]. Experimentally, the existence of an approximately linear relation between light intensity and swim velocity [19] allows to tune the motility and design spatial patterns with specific characteristics. Recent applications range from micro-motors [20,21] and rectification devices [22,23] to motility-ratchets [24]. Two experimental groups [25–27], have devised an intriguing technique to control the swimming speed of bacteria by using patterned light fields to enhance/reduce locally their motility by increasing/decreasing the light intensity. This leads to a consequent accumulation/depletion of particles in some regions, so that this procedure can be used to draw two dimensional images with the bacteria [25].

The fundamental physical concept behind experiments on light-controlled bacteria has been investigated many years ago in a theoretical context for noninteracting random walkers by Schnitzer [28] and later been extended to the interacting Run-and-Tumble model by Cates and Tailleur [29]: the lower the speed of active particles, the higher their local density. This theoretical result has been tested and confirmed in many numerical works and the existence of such a relation between particle velocity and density is now considered one of the most distinguishing features of active matter. A subsequent theoretical modeling of these effects has been proposed in Refs. [19, 30–33] by generalizing the active Brownian particle (ABP) model to include a spatially dependent swim velocity. This additional ingredient accounts for the well-known quorum sensing [34–36], chemotaxis and pseudochemotaxis [37–40] and correctly predicts a scaling of the density profile of individual particles with the inverse of the swim velocity. Including particle interactions in the ABP model may lead to the spontaneous formation of a membrane in two-step motility profiles [41] or cluster formation in regions with small activity [42]. Moreover, a temporal dependence in the activity landscape [43–48] may, in some cases, produce directed motion opposite to the propagation of the density wave [23,49].

The ABP model has been widely employed to obtain theoretical predictions [50–52] and

still represents one of the more spread active matter models for its versatility and broad applicability [53–58]. Nevertheless, the more recent active Ornstein-Uhlenbeck particle (AOUP) model [59–65], to be regarded as a "sister/brother" [66] of the ABP model, is generally easier to handle and often conveniently used to achieve further theoretical progress. For an ABP, the modulus of the active force is fixed and its orientation diffuses, while for an AOUP each component of the propulsion force evolves independently according to an Ornstein-Uhlenbeck process. Therefore, AOUPs can be used as an alternative to ABPs with simplified dynamics [67–69], to describe the behaviour of a colloidal particle in an active bath [70, 71]. Moreover, a convenient mapping between the parameters of the two models can be performed on the level of the autocorrelation function of the self-propulsion velocity [72, 73], such that their predictions agree fairly well for small and intermediate persistence time of the active motion [66]. The present authors recently modified the AOUP model to account for a spatially dependent swim velocity in Ref. [74] and obtained exact results for both the density profile and velocity distribution of a potential-free particle.

Analytical results for active particles in competing external potential and motility fields are sparse. Therefore, in this work, we extend the theoretical treatment from Ref. [74] by including the presence of an external force field, revealing more interesting properties than those obtained for constant swim velocity. For example, the density profile exhibits multiple peaks due to a competition between external forces and motility patterns, while the velocity distribution at fixed position displays a transition from a unimodal to a bimodal shape. The paper is structured as follows: In Sec. 2, we present the model to describe an active particle in a spatially dependent swim-velocity landscape and subject to an external potential, while, in Sec. 3, we develop our theoretical approach to describe the steady-state properties of such a system. The theory is numerically tested in Sec. 4 in the case of a harmonic potential and sinusoidal swim-velocity profile. Finally, conclusions and discussions are reported in Sec. 5. The appendices contain derivations and information supporting the theoretical treatment.

2 Model

2.1 Active particles with spatially dependent swim velocity

The position, $\mathbf{x}$, of an active particle evolves according to overdamped dynamics supplemented by a stochastic equation for the active driving, the so-called self-propulsion (or active) force, $\mathbf{f}_\mathrm{a}$. Such a force term is responsible for the persistence of the trajectory and its physical origin depends on the system under consideration: flagella for bacteria and chemical reactions for Janus particles, to mention just two examples. The active force $\mathbf{f}_\mathrm{a}$ can be written in the following form [66]:

$$\mathbf{f}_\mathrm{a} = \gamma v_0 \boldsymbol{\eta}\,, \tag{1}$$

where $\boldsymbol{\eta}$ is a stochastic process of unit variance, γ is the friction coefficient and v_0 is the constant swim velocity induced by the active force. To describe an active particle with a spatially dependent swim velocity, we employ the transformation $v_0 \to u(\mathbf{x}, t)$ in Eq. (1), which introduces a dependence on both position and time. The shape of $u(\mathbf{x}, t)$ must satisfy some properties related to physical arguments:

i) positivity: $u(\mathbf{x}, t) \geq 0$, for every $\mathbf{x}$ and t, since $u(\mathbf{x}, t)$ is the modulus of the velocity induced by the active force.

ii) boundedness: $u(\mathbf{x}, t)$ needs to be a bounded function of its arguments because the swim velocity cannot be infinite.

In what follows, we focus on the stochastic model introduced in Ref. [74], representing a generalization of the AOUP dynamics with $u(\mathbf{x},t)$.

Assuming inertial effects to be negligible at the microscopic scale, typically realized at small Reynolds numbers, the overdamped dynamics of the active particle with spatially modulating swim velocity reads:

$$\gamma\dot{\mathbf{x}} = \mathbf{F} + \gamma\sqrt{2D_\mathrm{t}}\boldsymbol{w} + \gamma u(\mathbf{x},t)\boldsymbol{\eta}\,, \tag{2a}$$

$$\tau\dot{\boldsymbol{\eta}} = -\boldsymbol{\eta} + \sqrt{2\tau}\boldsymbol{\chi}\,, \tag{2b}$$

where $\boldsymbol{\chi}$ and $\boldsymbol{w}$ are δ-correlated noises with zero average and unit variance and $\mathbf{F}$ is the force exerted on the particle, resulting from the gradient of a potential $U(\mathbf{x})$, i.e., $\mathbf{F}(\mathbf{x}) = -\nabla U(\mathbf{x})$. In this paper, we consider only a single particle, so that $U(\mathbf{x})$ is a one-body potential, but the description can be straightforwardly extended to the case of many interacting particles. The coefficient D_t is the translational diffusion coefficient due to the solvent satisfying the Einstein's relation with $D_\mathrm{t} = T_t/\gamma$ and the temperature, T_t, of the passive bath (for unit Boltzmann constant). The dynamics of $\boldsymbol{\eta}$ is characterized by the typical time, τ, which represents the correlation time of the active force autocorrelation and is usually identified with the persistence time of the single-trajectory, i.e., the time that a potential-free active particle spends moving in the same direction with velocity $u(\mathbf{x},t)$. In what follows, we neglect the contribution of the thermal bath by setting $D_\mathrm{t} = 0$, which is well justified in most of the experimental active systems [1].

By writing the active force in Eq. (2) as $\mathbf{f}_\mathrm{a}(\mathbf{x},t) = \gamma u(\mathbf{x},t)\boldsymbol{\eta}$ we have achieved two important goals. First, the spatial dependence of the self propulsion velocity can be conveniently accounted for through a multiplicative factor $u(\mathbf{x},t)$, which does not affect the dynamics of the noise vector. Therefore, in the absence of external or time dependent forces, we are able to analytically recover the law $\rho(\mathbf{x}) \sim 1/u(\mathbf{x})$ for the stationary density profile $\rho(\mathbf{x})$ [74], at variance with the alternative AOUP dynamics developed in Ref. [63] where such a law is reproduced only for profiles of $u(\mathbf{x})$ with slow spatial variation. As a consequence, our AOUP model is more suitable to describe the class of experimental systems for which the relation $\rho(\mathbf{x}) \sim 1/u(\mathbf{x})$ is observed, such as engineered E. Coli bacteria [25,27] or active colloids [19]. We expect that this consistency is also an advantage for describing interacting systems. Second, the Ornstein-Uhlenbeck process in Eq. (2b) has unit equal-time variance (except for a dimensional factor which we ignore here for convenience [73]), such that the reduced stationary probability distribution of $\boldsymbol{\eta}$ does not depend on the time scale τ. This means that $u(\mathbf{x})$ provides a unique velocity scale. Moreover, this unit-variance version of the AOUP model allows us to establish a direct link to the ABP model and an even larger family of models [66] for which Eq. (2a) has the same form. In turn, from Eq. (1) (or by taking $u(\mathbf{x},t) = v_0$), the standard version of the AOUP model is recovered by absorbing the velocity scale v_0 into the active diffusion coefficient $D_\mathrm{a} = v_0^2\tau$ (see also footnote [73] for a general discussion of the mapping between ABPs and the different versions of AOUPs in d spatial dimensions). From this identification, we see that the condition, $D_\mathrm{t} \ll D_\mathrm{a}$, necessary to neglect the thermal noise requires $u(\mathbf{x},t) > 0$, which is stronger than the one stated above.

2.2 Velocity description of an active Ornstein-Uhlenbeck particle (AOUP)

Our equation of motion (2a) of an AOUP with a spatially dependent swim velocity contains a multiplicative colored noise, which does not readily allow us to gain further analytic insight. As a first step to ease the theoretical treatment of our model, we switch to the auxiliary dynamics employed earlier in the potential-free case [74]. Instead of describing the system in terms of position $\mathbf{x}$ and self-propulsion velocity $u(\mathbf{x})\boldsymbol{\eta}$, we take advantage of the relation (holding for $D_\mathrm{t} = 0$)

$$\gamma\dot{\mathbf{x}} = \mathbf{F} + \gamma u(\mathbf{x},t)\boldsymbol{\eta} \tag{3}$$

to perform the simple change of variables $(\mathbf{x}, \boldsymbol{\eta}) \to (\mathbf{x}, \dot{\mathbf{x}} = \mathbf{v})$. This trick allows us to directly study the position and the velocity of the active particle as for $u(\mathbf{x}, t) = v_0$. As in the potential-free case, to return to the original variables, we need to account for the space-dependent Jacobian matrix $\mathcal{J}$ of the transformation reported in Appendix A. The resulting Jacobian reads:

$$\det[\mathcal{J}] = u(\mathbf{x}, t)\,, \tag{4}$$

where $\det[\cdot]$ represents the determinant of a matrix. Therefore, the probability distributions, $\tilde{p}(\mathbf{x}, \boldsymbol{\eta}, t)$ and $p(\mathbf{x}, \mathbf{v}, t)$, in the two coordinate frames satisfy the following relation:

$$\tilde{p}(\mathbf{x}, \boldsymbol{\eta}, t) = \det[\mathcal{J}]\, p(\mathbf{x}, \mathbf{v}, t)\,. \tag{5}$$

Note that the condition $u(\mathbf{x}, t) > 0$ implies $\det[\mathcal{J}] > 0$ and, thus guarantees the possibility of performing the transformation. In what follows, we use these new variables to study a system subject to both a spatially dependent swim velocity, $u(\mathbf{x}, t)$, and an external potential $U(\mathbf{x})$. The generalization to include a thermal noise can be achieved by following Ref. [75].

To derive the dynamics in the variables $\mathbf{x}$ and $\mathbf{v}$, we adopt a simple strategy whose leading steps are reported in details in Appendix A. We perform the time-derivative of Eq. (3), substitute $\dot{\boldsymbol{\eta}}$ with Eq. (2b) and then replace $\boldsymbol{\eta}$ with $\mathbf{v}$ and $U(\mathbf{x})$, using again Eq. (3), and finally obtain an equivalent equation of motion for the velocity $\mathbf{v}$. The full result reads

$$\dot{\mathbf{x}} = \mathbf{v}\,, \tag{6a}$$

$$\begin{aligned}\gamma\tau\dot{\mathbf{v}} = &-\gamma\boldsymbol{\Gamma}(\mathbf{x})\cdot\mathbf{v} - \nabla U + \gamma u(\mathbf{x}, t)\sqrt{2\tau}\,\boldsymbol{\chi} \\ &+ \tau\frac{[\gamma\mathbf{v} + \nabla U]}{u(\mathbf{x}, t)}\left(\frac{\partial}{\partial t} + \mathbf{v}\cdot\nabla\right)u(\mathbf{x}, t)\,.\end{aligned} \tag{6b}$$

In Eq. (6b), the first line is identical to the expression describing the constant case $u(\mathbf{x}, t) = v_0$: the dynamics of an overdamped active particle is mapped onto that of an underdamped passive particle with a spatially dependent friction matrix, $\gamma\boldsymbol{\Gamma}(\mathbf{x})$, which depends on the second derivatives of the potential and reads:

$$\boldsymbol{\Gamma}(\mathbf{x}) = \mathbf{I} + \frac{\tau}{\gamma}\nabla\nabla U(\mathbf{x})\,, \tag{7}$$

where $\mathbf{I}$ is the identity matrix. Such a term increases or decreases the effective particle friction according to the value of the curvature of $U(\mathbf{x})$, which becomes more and more important as τ becomes large. In addition, as already found in the potential-free case, the noise amplitude contains a spatial and temporal dependence through the multiplicative factor $u(\mathbf{x}, t)$. The second line of Eq. (6b) contains the new terms, absent for $u(\mathbf{x}, t) = v_0$, accounting for both the time- and space-dependence of $u(\mathbf{x}, t)$.

For a further discussion of the new terms arising from a modulating swim-velocity profile, we restrict ourselves to the time-independent case, $u(\mathbf{x}, t) = u(\mathbf{x})$. Then, we identify two contributions to the total force. The first one, $\propto \mathbf{v}\mathbf{v}\cdot\nabla u$, is proportional to the square of the velocity and appears also in the absence of an external potential. Since it is even under time-reversal transformation, it cannot be interpreted as an effective Stokes force. The second force, $\propto (\nabla U)\mathbf{v}\cdot\nabla u$, couples the gradients of the potential and the swim velocity and gives rise to an extra space-dependent contribution to the effective friction. This allows us to absorb this term into a generalized effective friction matrix $\boldsymbol{\Lambda}(\mathbf{x})$, which reads:

$$\boldsymbol{\Lambda}(\mathbf{x}) = \boldsymbol{\Gamma}(\mathbf{x}) + \frac{\tau}{\gamma}\mathbf{F}(\mathbf{x})\frac{\nabla u(\mathbf{x})}{u(\mathbf{x})}\,, \tag{8}$$

where $\boldsymbol{\Gamma}(\mathbf{x})$ is given by the expression for constant $u(\mathbf{x}) = v_0$ (see Eq. (7)). The new term in Eq. (8) linearly increases with increasing τ and provides a further spatial dependence to

the friction matrix. Its sign is determined by $\nabla u(\mathbf{x})$ and $\mathbf{F}(\mathbf{x}) = -\nabla U(\mathbf{x})$, such that it can increase (positive sign) or decrease (negative sign) the effective friction. As a matter of fact, the spatial modulation of the swim velocity and the action of an effective potential are two distinct physical phenomena, which cannot be simply mapped onto each other. Indeed, $u(\mathbf{x})$ provides an additional contribution to the effective friction in the dynamics of $\mathbf{v}$ but does not give any contributions to the confining force, at variance with the potential $U(\mathbf{x})$ that affects both the force acting on the particle and the effective friction matrix (see footnote [76] for an explicit example with a detailed discussion of the physical implications). Moreover, the interplay between the gradients of both fields in the second term of Eq. (8) gives rise to nontrivial physical effects that will be investigated in the following.

3 Theoretical predictions

3.1 Approximate stationary distributions

So far, all steps in Sec. 2.2 were exact and the drawn conclusions general. To make further theoretical progress, we continue to restrict ourselves to a static swim-velocity profile $u(\mathbf{x})$. At variance with the potential-free case, $U(\mathbf{x}) = 0$, the exact steady-state probability distribution of positions and velocities, $p(\mathbf{x}, \mathbf{v})$, is unknown and one needs to resort to approximations. To this end, we assume that all components of the probability current vanish, as in the case of a homogeneous swim velocity, $u(\mathbf{x}) = v_0$. As shown in Appendix B, this condition means that in the Fokker-Planck equation associated to Eq. (6) the effective drift and diffusive terms mutually balance. To derive a closed expression for the spatial density $\rho(\mathbf{x})$, we follow in Appendix B the idea of Hänggi and Jung behind the Unified Colored Noise Approximation (UCNA) [77–79]: having derived the auxiliary dynamics (6), where the colored noise $\boldsymbol{\eta}$ is replaced by a white noise $\boldsymbol{\chi}$, we formally identify a new variable $\dot{\mathbf{z}} := \dot{\mathbf{x}}/u(\mathbf{x})$ to eliminate the multiplicative nature of the noise and then neglect the generalized inertial term $\propto \ddot{\mathbf{z}}$ in Eq. (6b). This procedure yields an effective overdamped equation for the particle position $\mathbf{x}$ and finally, via the associated Smoluchowski equation for the time evolution of $\rho(\mathbf{x}, t)$, the stationary density distribution $\rho(\mathbf{x})$ for a system with space-dependent activity. Our theoretical method employs the vanishing-currents approximation and, as a consequence, allows us to derive an effective equilibrium theory whose validity will be investigated numerically. In the absence of thermal noise, the same (stationary) $\rho(\mathbf{x})$ can be obtained using the path-integral method proposed by Fox [80,81]. As already shown in the case of homogeneous swim velocity, both the UCNA and the Fox approach give rise to the exact distribution in the small-persistence regime, i.e., when the persistence time is smaller than the other typical times characterizing the dynamics, while they only capture the qualitative behavior of the system in the opposite regime (i.e., when the persistence time is comparable or larger than the other relevant time scales). In particular, in the present case, τ needs to be compared to both the relaxation time due to the potential and to the typical time induced by the spatial modulation of the swim-velocity profile (see Sec. 4.1 for an explicit discussion in the specific case of a harmonic oscillator).

Here, we report only the main results while the details of the derivation can be found in Appendix B. The whole stationary probability distribution reads:

$$p(\mathbf{x}, \mathbf{v}) \approx \rho(\mathbf{x}) \frac{\sqrt{\det[\boldsymbol{\Lambda}(\mathbf{x})]}}{\sqrt{2\pi} u(\mathbf{x})} \exp\left(-\frac{\mathbf{v} \cdot \boldsymbol{\Lambda}(\mathbf{x}) \cdot \mathbf{v}}{2u^2(\mathbf{x})}\right). \tag{9}$$

We remark that the prefactor $\sqrt{\det[\boldsymbol{\Lambda}(\mathbf{x})]}/(\sqrt{2\pi} u(\mathbf{x}))$ is the explicit factor normalizing the conditional velocity distribution (i.e., at fixed position $\mathbf{x}$). The function $\rho(\mathbf{x})$ is approximated

by

$$\rho(\mathbf{x}) \approx \frac{\mathcal{N}}{u(\mathbf{x})}\det[\mathbf{\Lambda}(\mathbf{x})]\exp\left(\frac{1}{\gamma\tau}\int^{x} d\mathbf{y}\cdot\frac{\mathbf{\Lambda}(\mathbf{y})\cdot\mathbf{F}(\mathbf{y})}{u^2(\mathbf{y})}\right) \tag{10}$$

with $\mathcal{N}$ being a normalization constant. Our expression for $\rho(\mathbf{x})$ coincides with the spatial density because it follows from integrating out the velocity in Eq. (9). The full distribution (9) displays a multivariate Gaussian profile in the velocity, whose covariance matrix accounts for the nontrivial coupling between velocity and position:

$$\langle \mathbf{v}\mathbf{v}(\mathbf{x})\rangle = u^2(\mathbf{x})\mathbf{\Lambda}^{-1}(\mathbf{x})\,. \tag{11}$$

The covariance $\langle \mathbf{v}\mathbf{v}(\mathbf{x})\rangle$ is spatially modulated by $u(\mathbf{x})$, which also occurs in the potential-free case, so that, in the regions where the swim velocity is large, the particle moves faster. Moreover, the external potential not only affects the velocity covariance through $\mathbf{\Gamma}(\mathbf{x})$, as in the case $u(\mathbf{x}) = v_0$ (see for instance Refs. [82, 83]), but contains an additional spatial dependence through the coupling to the velocity gradient in the second term of Eq. (8).

We remark that a necessary condition to obtain predictions (9) and (10) (and, consequently, (11)) is that the matrix $\mathbf{\Lambda}$ is positive definite, so that its inverse exists. This is the main limitation of our theoretical approach, which is always suitable to describe the system in the small-persistence regime (when τ is small compared to the other relevant time scales), but can break apart in the large-persistence regime where the position-dependent part of the matrix $\mathbf{\Lambda}(\mathbf{x})$ becomes dominant (with respect to $\mathbf{I}$). As a consequence, our approach is supposed to work (at least qualitatively) in any spatial dimension and for every value of τ if (i) $U(\mathbf{x})$ is a convex function, (ii) $U(\mathbf{x})$ depends on a single Cartesian coordinate or has a positive slope in a radial geometry and (iii) the gradients of $U(\mathbf{x})$ and $u(\mathbf{x})$ enclose a sufficiently large angle $\alpha \geq \pi/2$. The requirements (i) and (ii) correspond to a positive definiteness of $\mathbf{\Gamma}(\mathbf{x})$, given in Eq. (7), and are thus already necessary for $u(\mathbf{x}) = v_0$ [72], while (iii) arises in addition from the second term in Eq. (8). If the two functions $U(\mathbf{x})$ and $u(\mathbf{x})$ violate either of the three conditions (i-iii), our predictions cannot qualitatively reproduce the behavior of a system for large enough τ.

Since the distribution $\rho(\mathbf{x})$ from Eq. (10) can be interpreted as the effective density distribution of the system, the particle behaves as if it was subject to an effective potential, $\mathcal{V}(\mathbf{x}) := -\tau\gamma v_0^2 \ln(\rho(\mathbf{x}))$, which explicitly reads:

$$\mathcal{V}(\mathbf{x}) = -v_0^2\int^{x} d\mathbf{y}\cdot\frac{\mathbf{\Lambda}(\mathbf{y})\cdot\mathbf{F}(\mathbf{y})}{u^2(\mathbf{y})} - \tau\gamma v_0^2\ln\left(v_0\frac{\det[\mathbf{\Lambda}(\mathbf{y})]}{u(\mathbf{x})}\right) \tag{12}$$

up to a constant. This expression contains two terms, i) the spatial integral of the external force modulated by the inverse of the covariance matrix of the velocity distribution, cf. Eq. (11), and ii) the logarithm containing both the velocity modulation $u(\mathbf{x})$ and the determinant of the position-dependent matrix $\mathbf{\Lambda}^{-1}(\mathbf{x})$. For a constant swim velocity, $u(\mathbf{x}) = v_0$, we can perform the integral explicitly and the effective potential $\mathcal{V}(\mathbf{x})$ reduces to the known closed form found within the standard UCNA or Fox approach [72] since we neglect translational Brownian noise. Note that the spatial dependence of the swim velocity gives rise to an additional potential term with respect to the case $u(\mathbf{x}) = v_0$ contained in the expression for $\mathbf{\Lambda}(\mathbf{x})$. At equilibrium, when $u(\mathbf{x}) = v_0$ and $\tau \to 0$, the density reduces to the well known Maxwell-Boltzmann profile, since $\mathbf{\Lambda}(\mathbf{x})$ becomes unity.

3.2 Multiscale method for the full-space distribution

To check the validity of our predictions, at least in the small-persistence regime, we resort to an exact perturbative approach in powers of the persistence time τ. For simplicity, the technique

is presented in the one-dimensional case because the generalization to higher dimensions is technically more involved and does not provide additional insight. In addition, as in experiments based on active colloids [19], we will consider a one-dimensional swim-velocity profile $u(x)$ in the remainder of this work, justifying our particular attention to the one-dimensional case in the following presentation.

Our starting point is the following Fokker-Planck equation for the probability distribution $p(x,v,t)$:

$$\partial_t p = \frac{\Lambda(x)}{\tau}\frac{\partial}{\partial v}(vp) + \frac{u^2(x)}{\tau}\frac{\partial^2}{\partial v^2}p - \frac{F(x)}{\tau\gamma}\frac{\partial}{\partial v}p - v\frac{\partial}{\partial_x}p - \frac{1}{u(x)}\left(\frac{\partial}{\partial x}u(x)\right)\frac{\partial}{\partial v}\left(v^2 p\right), \quad (13)$$

associated to the dynamics (6) in one spatial dimension. Its solution is unknown for a general potential $U(x)$, even in the special case $u(x) = v_0$. Therefore, one needs to resort to approximation methods or perturbative strategies to obtain analytical insight. As shown in previous works [84, 85], it is possible to obtain perturbatively both the full distribution $p(x,v,t)$ and the configurational Smoluchowski equation for the reduced space distribution $\rho(x,t)$ following the method developed by Titulaer in the seventies [86]: starting from the Fokker-Planck equation (13) the velocity degrees of freedom can be eliminated by using a multiple-time-scale technique. Physically speaking, the fast time scale of the system corresponds to the time interval necessary for the velocities of the particles to relax to the configurations consistent with the values imposed by the vanishing of the currents. The characteristic time of the slow time scale is much longer and corresponds to the time necessary for the positions of the particles to relax towards the stationary configuration.

In the present case, the perturbative parameter is the persistence time τ. Since we are mainly interested in time-independent properties, we limit ourselves to compute the steady-state probability distribution by generalizing the results of Refs. [87, 88] previously obtained for the case $u(x) = v_0$ (see also Ref. [89] for a more general expansion with an additional thermal noise). For space reasons, the details of the calculations are reported in Appendix C. Our main result is the following exact perturbative expansion of the distribution $p(x,v)$ in powers of the parameter τ: [90]

$$\begin{aligned} p(x,v) = \rho_s(x)p_s(x,v)\Bigg\{1 + \frac{\tau}{\gamma}\Big[\frac{1}{2}U''(x) - \frac{v^2}{2u^2(x)}U''(x) + \left(\frac{v^2}{2u(x)^2} - \frac{1}{2}\right)U'(x)\frac{u'(x)}{u(x)}\Big] \\ + \frac{\tau^2}{6\gamma}u(x)\left(\frac{v^3}{u^3(x)} - 3\frac{v}{u(x)}\right)\left[U'''(x) - \frac{\partial}{\partial x}\left(\frac{U'(x)}{u(x)}u'(x)\right)\right]\Bigg\} + O(\tau^3) \end{aligned} \quad (14)$$

where the normalized distribution $p_s(x,v)$ is given by

$$p_s(x,v) = \frac{\mathcal{N}}{\sqrt{2\pi}u(x)}\exp\left(-\frac{v^2}{2u^2(x)}\right), \quad (15)$$

and the function $\rho_s(x)$ reads

$$\rho_s(x) = \mathcal{N}\frac{\Lambda(x)}{u(x)}\exp\left(-\frac{1}{\gamma\tau}\int^x dy\, U'(y)\frac{\Lambda(y)}{u^2(y)}\right). \quad (16)$$

with the normalization factor $\mathcal{N}$ and the prime as a short notation for the spatial derivative. Already at order τ/γ our general result (14) for a nonuniform swim velocity contains an extra term proportional to $\partial_x u(x)$, compared to the expansion derived in Ref. [87, 88, 90], which is responsible for an additional coupling between position and velocity.

The product $\rho_s(x) \times p_s(x,v)$ in Eq. (14) plays the role of an effective equilibrium-like distribution, which is exact in the limit $\tau \to 0$. The required expression (15) for $p_s(x,v)$ is the

exact solution of the potential-free active system with a spatially dependent swim velocity as derived in Ref. [74]: it is a Gaussian probability distribution for the particle velocity v with an effective position-dependent kinetic temperature provided by $u^2(x)$. The spatial density $\rho_s(x)$ from Eq. (16) corresponds to the UCNA result (10) in one dimension. Our previous approximated expression (9) for $p(x,v)$ is consistent with the full result (14) at first order in the expansion parameter $\propto \tau$. The first deviation between the two formulas occurs at order $O(\tau^2)$, where the exact expression for $p(x,v)$ contains additional odd terms in v. The exact density profile $\rho(x) = \int \mathrm{d}v p(x,v) = \rho_s(x) + O(\tau^2)$ deviates from the UCNA result beyond linear orders in τ. As a consequence, we expect that our UCNA approximation, $\rho_s(x)$, is exact in the small-persistence regime, while it could only reproduce the qualitative behavior of $\rho(x)$ in the large-persistence regime.

4 The harmonic oscillator

4.1 Swim-velocity profile and external potential in one dimension

In this section, we present and investigate the interplay between a spatially modulated swim velocity and an external confining potential in one spatial dimension. While, in Sec. 3.2, we have shown that our analytical predictions from Eqs. (9), (10) and (11) are exact in the small-persistence regime through analytical arguments, a numerical analysis is necessary to check our approximations in the large-persistence regime.

To fix the form of the profile $u(x)$ employed in our numerical study and theoretical treatment, we take inspiration from experimental works on active colloids [19] and consider a static periodic profile $u(x)$ varying along a single direction, namely the x axis, so that:

$$u(x) = v_0\left(1 + \alpha\cos\left(2\pi\frac{x}{S}\right)\right), \tag{17}$$

where $\alpha < 1$ and $v_0 > 0$ so that $u(x) > 0$ for every x. The parameter α determines the amplitude of the swim velocity oscillation while $S > 0$ sets its spatial period. As a consequence, the active particle is subject to the minimal swim velocity $v_0(1-\alpha)$ and to the maximal one $v_0(1+\alpha)$. This choice and the features of the AOUP allow us to consider directly a one-dimensional system, essentially focusing only on the x component and neglecting the dynamics of the other spatial coordinates.

We remind that, in the potential-free case [56], the system admits two typical length scales, i.e., the persistence length $v_0\tau$ and the spatial period, S, of the swim-velocity profile (17). In other words, by rescaling the time by τ and the particle position by $v_0\tau$, the dynamics is controlled by the dimensionless parameter $v_0\tau/S$ and by the dimensionless parameter α quantifying the amplitude of the swim-velocity oscillation. The external force $F(x)$ then introduces at least one additional length-scale, ℓ, which depends on the specific nature of F, and, thus, an additional dimensionless parameter, say $\ell/(v_0\tau)$, related to the external potential. The last dimensionless parameter controls the dynamics also in the case $u(x) = v_0$ [91]. Now, we can identify the small-persistence regime, where the self-propulsion velocity relaxes faster than the particle position, with the criterion $v_0\tau/S \ll 1$ and $\ell/(v_0\tau) \gg 1$. Under the former condition, we expect that the system behaves as its passive counterpart: if $\tau \ll S/v_0$ holds, the self-propulsion behaves as an effective white noise. In the opposite case, when $v_0\tau/S \gg 1$, the dynamics is strongly persistent and we expect intriguing nonequilibrium properties.

Now, we confine the particles through a harmonic potential,

$$U(x) = \frac{k}{2}x^2, \tag{18}$$

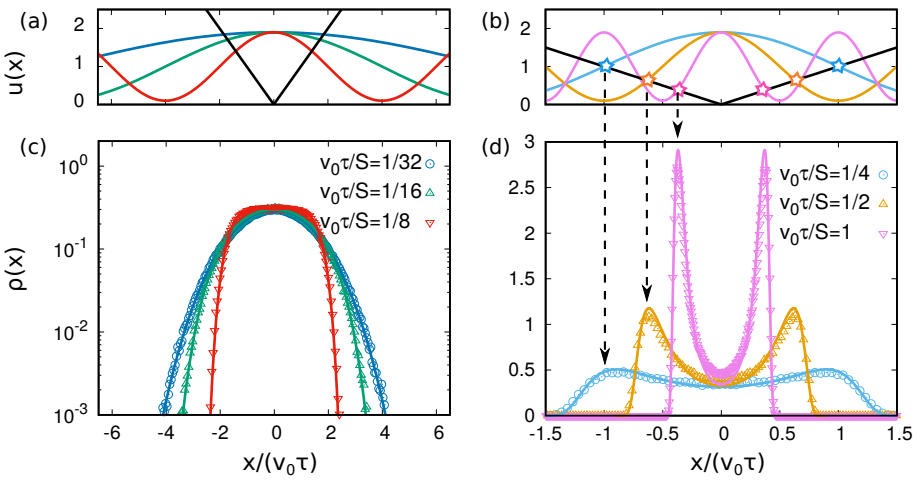

Figure 1: Density distributions. Panels (a) and (b): swim-velocity profile $u(x)$ for different values of S (colored curves), compared with the modulus of the linear force profile, $|F(x)| = -k|x|/\gamma$ (black curve) as a reference. The colored stars are placed at the first cross point between $u(x)$ and $F(x)/\gamma$. Panels (c) and (d): spatial density profile, $\rho(x)$, for different values of S. Points are obtained by numerical simulations while solid lines by plotting the theoretical prediction (10) (that reduces to Eq. (16) in one dimension with $\Lambda(x)$ given by Eq. (19)). The integral occurring in Eq. (16) has been performed numerically. Panels (a), (c) and (b), (d) share the same legend. Simulations are realized in one spatial dimension with $\tau k/\gamma = 1$ and $\alpha = 0.9$.

where the constant k determines the strength of the linear force. The dimensionless parameter associated with this external potential is thus $k\tau/\gamma$, i.e., $\ell = v_0\tau^2 k/\gamma$. By observing that the curvature of the potential is constant, the effective friction coefficient $\Lambda(x)$ from Eq. (8) becomes:

$$\Lambda(x) = \left(1 + \tau\frac{k}{\gamma}\right)\left(1 + \frac{\alpha x}{u(x)^2}\frac{2\pi}{S}\sin\left(2\pi\frac{x}{S}\right)\frac{\tau\frac{k}{\gamma}}{1+\tau\frac{k}{\gamma}}\right). \tag{19}$$

As shown by Eq. (19), the two dimensionless parameters $\tau k/\gamma$ and α play a similar role. Indeed, they only determine the relative amplitude of the spatial modulation of $\Lambda(x)$. When either α or $\tau k/\gamma$ vanish, the effective friction becomes constant and the coupling between velocity and position disappears. Instead, when we approach both limits $\tau k/\gamma \to \infty$ and $\alpha \to 1$, the amplitude of the spatial oscillations becomes maximal. By varying the dimensionless parameter $v_0\tau/S$, on the other hand, one can explore the different properties of the system: when $v_0\tau/S$ grows, the spatial period of $u(x)$ decreases and the position-dependent term of $\Lambda(x)$ becomes less relevant. To study the resulting behavior of the system in detail, we keep fixed $\alpha = 0.9$ and $\tau k/\gamma = 1$ and we change only $v_0\tau/S$ to study the properties of the system.

4.2 Density distribution

To understand the peculiar behavior of an AOUP with spatial modulation (17) of the swim velocity and confined in a harmonic trap (18), we first focus in Figs. 1 and 2 on the spatial density profile, $\rho(x)$. The bottom panels show $\rho(x)$ for different values of the spatial period S (through the dimensionless parameter $v_0\tau/S$) of the swim velocity $u(x)$, which we compare in the top panels to the modulus $|F(x)|/\gamma$ of the confining force $F(x) = -U'(x)$ as a reference.

In the small-persistence regime, $v_0\tau/S \ll 1$ (see panels (a) and (c) of Fig. 1), the unimodal density distribution is fairly described by expanding the UCNA solution (10) in powers of x/S,

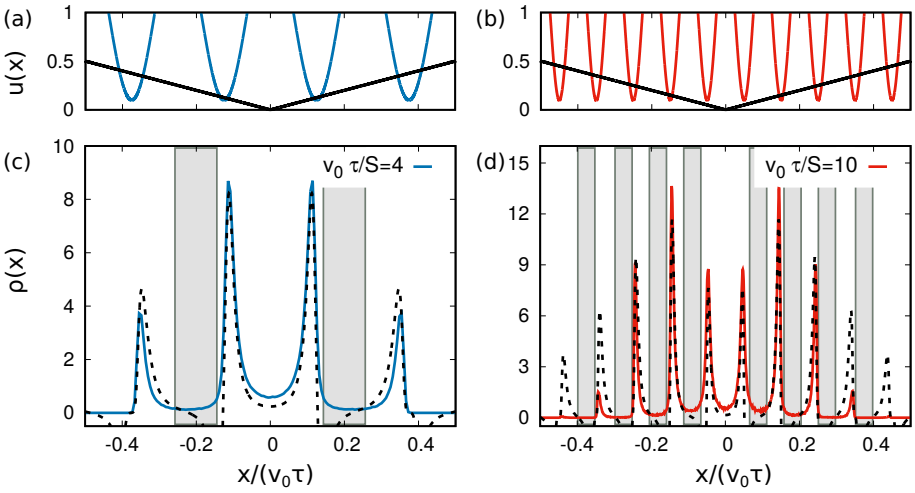

Figure 2: Density distributions. Panels (a) and (b): swim-velocity profile $u(x)$ for two different values of S (colored curves), compared with the modulus of the linear force profile, $|F(x)| = -k|x|/\gamma$ (black curve) as a reference. Panels (c) and (d): spatial density profile, $\rho(x)$, for different values of S. Solid colored lines (blue in panel (c) and red in panel (d)) are obtained by numerical simulations while dashed black lines by plotting the theoretical prediction (10) (that reduces to Eq. (16) in one dimension with $\Lambda(x)$ given by Eq. (19)). The integral occurring in Eq. (16) has been performed numerically. Grey rectangles are drawn in the regions where Eq. (10) is not defined, say when $\Lambda(x) < 0$ (see the main text for more details). Panels (a), (c) and (b), (d) share the same legend. Simulations are realized in one spatial dimension with $\tau k/\gamma = 1$ and $\alpha = 0.9$.

obtaining:

$$\rho(x) \sim \exp\left(-\frac{1+\tau\frac{k}{\gamma}}{(1+\alpha)^2}\frac{k}{v_0^2}\frac{x^2}{2}\right). \tag{20}$$

In the expression (20), we have neglected the terms proportional to x^2/S^2, x^4/S^2 and all higher-order terms in power of $\sim 1/S$. Remarkably, even in this crude approximation, we see from the factor $(1+\alpha)^2$ that the oscillations of the swim velocity lead to a decrease of the second moment $\langle x^2\rangle$ of $\rho(x)$ compared to the homogeneous case $u(x) = v_0$. This prediction is consistent with previous results obtained in the absence of an external potential, where the swim-velocity oscillations produce the decrease of the long-time diffusion coefficient [74] (see also Ref. [92]). In this regime, the spatial pattern $u(x)$ produces an effective potential with increasing stiffness for increasing spatial modulation. For higher $v_0\tau/S$, the distribution starts developing non-Gaussian tails, which are still well-described by including higher-order terms in the UCNA expansion (20).

When increasing $v_0\tau/S$ further (see panels (b) and (d) of Fig. 1), $\rho(x)$ becomes a bimodal distribution with two peaks symmetric to the origin, as in a system confined in a double-well potential. This effect is absent in the case $u(x) = v_0$ where the AOUP density distribution in a harmonic potential always has a Gaussian shape [60, 93–95]. For a position-dependent swim velocity, the comparison between the analytical result (10) (that reduces to Eq. (16) in one dimension) and the numerical simulations still reveals a good agreement: in particular, Eq. (10) is able to predict the observed bimodality of the distribution. To explain the occurrence of this bimodality in the shape of $\rho(x)$, we can use an effective (but rather general) force-balance argument in Eq. (2a). This argument can be applied to the present intermediate-persistence regime, $v_0\tau/S \sim 1$ (or also for $v_0\tau/S \gg 1$ discussed later), where the self-propulsion vector η

in the active force can be considered to be roughly constant for typical times $t \lesssim \tau$. Since the variance of η is unitary, the most likely value assumed by the self-propulsion velocity at point x is simply $u(x)$ (in absolute value). For this reason, it is generally unlikely to find the particle in regions with $u(x) < |F(x)|/\gamma$, because there the particle's self propulsion is not sufficient to climb up the potential gradient. Moreover, in the spatial points where $u(x) > |F(x)|/\gamma$, the active particle does not get stuck on average because its high self-propulsion velocity allows for its directed motion until $u(x) = |F(x)|/\gamma$ is fulfilled. When this force balance occurs, the particle can explore further spatial regions only because of large (and rare) fluctuations of η. This reasoning is confirmed by inspecting Fig. 1 for different fixed values of $v_0\tau/S$. It is evident from the dashed arrows that the peaks of the distribution in Fig. 1(d) coincide with the intersection between the modulus $|F(x)|/\gamma$ of the external force (black curve) and $u(x)$ (colored curves) in Fig. 1(c).

Starting from the theoretical result (10), we can predict the critical value S_c at which the distribution becomes bimodal, by simply requiring that $\mathrm{d}^2/\mathrm{d}x^2\rho(x) = 0$ (at $x = 0$), obtaining:

$$\frac{S_c^2}{v_0^2\tau^2} = (2\pi)^2\alpha(1+\alpha)\left[\frac{1+3\tau\frac{k}{\gamma}}{\left(1+\tau\frac{k}{\gamma}\right)^2}\right]\frac{\gamma}{k\tau}\,. \tag{21}$$

In general, we predict that the value of $S_c/(v_0\tau)$ increases with increasing α (recall that $0 < \alpha < 1$) and is a decreasing function of $\tau k/\gamma$. This is consistent with our physical intuition: larger oscillations (i.e., larger α) facilitate the transition to a bimodal shape. Indeed, the larger α, the smaller the minimal self-propulsion velocity, that hinders the particle's ability to come back to the origin. Instead, the increase of $\tau k/\gamma$ gives rise to the opposite behavior: the larger $\tau k/\gamma$, the steeper the effective confining trap. As a consequence, the active particle needs larger fluctuations of η to reach spatial regions where $u(x)$ assumes low values which compete with the external force. Specifically, for the chosen parameters $\alpha = 0.9$ and $\tau k/\gamma = 1$, Eq. (21) predicts the onset of bimodality for $v_0\tau/S > 1/8$. From Fig. 1, we also observe that the increase of $v_0\tau/S$ beyond this threshold enhances the bimodality showing two symmetric peaks with increasing height but occurring at spatial positions which get closer.

In the large-persistence regime $v_0\tau/S \gg 1$ (see Fig. 2), we observe the emergence of many symmetric peaks in $\rho(x)$. Their positions are still determined by the balance between $u(x)$ and $|F(x)|/\gamma$, and, in this case, roughly coincide with the minima of $u(x)$ close to the origin (i.e., the minimum of $U(x)$). As shown in Fig. 2 (a), $u(x)$ first crosses $|F(x)|/\gamma$ almost in its first minima (at $x/v_0\tau \approx \pm 0.15$) for $v_0\tau/S = 4$. This implies that small fluctuations of the self-propulsion velocity allows the particle to explore spatial regions which are even more distant from the potential minimum, so that it also accumulates at the second crossing point (at $x/v_0\tau \approx 0.4$). According to Fig. 2 (c), the height of these secondary peaks is smaller than that of the primary ones because the particle remains trapped at the first balance points for most of the time, while only on rare occasions its swim velocity is sufficient to further climb up the potential gradient. In Fig. 2 (d), for an even larger value of $v_0\tau/S = 10$, we observe that the height of the peaks near the origin is lower than that of the successive peaks. In this case, Fig. 2 (b) shows that the minima of $u(x)$ closest to the origin are still larger than $|F(x)|/\gamma$, so that (most of the time) the particle has a sufficiently large self-propulsion velocity to go further until entering the spatial region where the first intersection of $u(x)$ and $|F(x)|/\gamma$ occurs. We conclude that, even in the case of a harmonic potential, the oscillation of the swim velocity allows the AOUP to climb up the potential barrier and accumulate preferredly in spatial regions (corresponding to minima of $u(x)$), which are further away from the origin.

Finally, we note that in the large-persistence regime, the UCNA prediction (10) (or Eq. (16) in one-dimension) for the spatial distribution fails. This occurs because of the presence of spatial regions where the effective friction $\Lambda(x)$, given by Eq. (19), becomes negative (see the

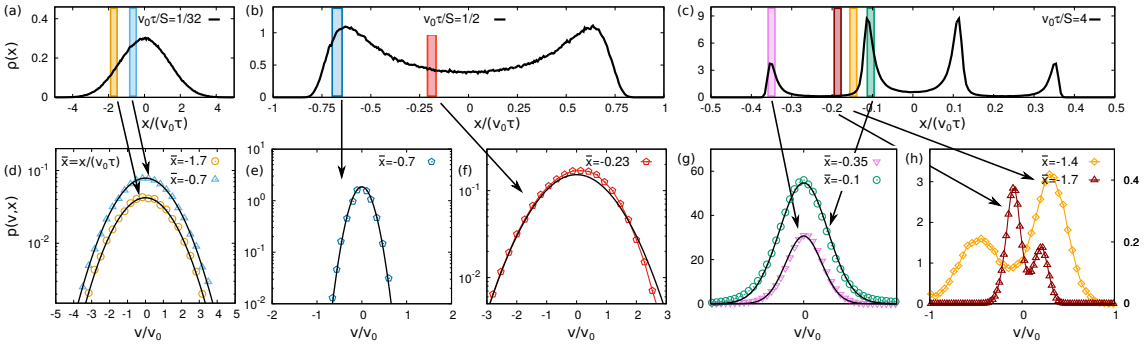

Figure 3: Velocity distributions. Panels (a), (b) and (c): simulated density distribution $\rho(x)$ for $S/(v_0\tau) = 32, 2, 1/4$, respectively, as a reference. Colored rectangles are drawn in correspondence of the spatial regions used to calculate the velocity distribution in the other panels. Panels (d), (e), (f), (g) and (h): velocity distribution $p(v,x)$ as a function of v calculated at fixed positions $x = \bar{x}v_0\tau$ according to the legend. Panel (d) is calculated at $S = 32$, panels (e) and (f) at $S = 2$ and panels (g) and (h) at $S = 0.25$. Colored symbols and lines are obtained by numerical simulations and solid black lines show the theoretical prediction (9) if applicable (the theory yields a one-dimensional Gaussian and requires a positive definiteness of $\Lambda(x)$ given by Eq. (19)). Simulations are realized in one spatial dimension with $\tau k/\gamma = 1$ and $\alpha = 0.9$.

gray-shaded regions in Fig. 2(c) and (d)). This implies that also the corresponding approximation for $\rho(x)$ can assume negative values. This failure resembles the one of the UCNA (or the Fox approach) for the standard AOUP model with $u(x) = v_0$ confined in a nonconvex potential [72]. In that case, the strongly non-Gaussian nature of the system is at the basis of new intriguing phenomena, such as the occurring of effective negative mobility regions [96], the overcooling of the system [97] and the violation of the Kramers law for the escape properties [98, 99]. We expect that our model could display a similar phenomenology and that such problems can be treated by using similar theoretical techniques [96, 100–102]. However, we stress that the generalized UCNA still accurately predicts the positions of the main peaks in Fig. 2 (c), although in Fig. 2 (d) there emerge additional smaller peaks further away from the origin, which are absent in simulations. The appearance of those fake peaks is reminiscent of the overestimated wall accumulation predicted by UCNA for $u(x) = v_0$.

4.3 Velocity distribution

We now focus on the dependence of the full joint probability density $p(x,v)$ on the velocity, shown in Fig. 3 for some representative values of the particle's position x. Moreover, we choose three different values of $S/(v_0\tau)$ to explore the three distinct regimes observed in Sec 4.2. For each regime, we report once again the density distribution $\rho(x)$ in panels (a), (b) and (c), where colored bars mark the regions for which we calculate $p(x,v)$ as a function of v in panels (d), (e), (f), (g), (h).

In the regime of small persistence, $(v_0\tau)/S \ll 1$, the shape of $p(v,x)$ is Gaussian, independently of the position x (Fig. 3 (d)). This result fully agrees with the prediction (9) (that simply reduces to a one-dimensional Gaussian) as revealed by the comparison between colored data points and black solid lines in Fig. 3 (d). As predicted by the position-dependent variance in Eq. (11), different positions x come along with a change in the width of the velocity distribution.

In Fig. 3 (e) and (f), the regime of intermediate persistence, $v_0\tau/S \sim 1$, is investigated,

which displays a bimodality in the density distribution. Here, we compare $p(x,v)$ calculated in the vicinity of a peak of $\rho(x)$ to the velocity profile near the local minimum of $\rho(x)$ (close to the origin). In the former case, the distribution $p(x,v)$ displays an almost Gaussian shape in agreement with Eq. (9), while in the latter case, it deviates from the theoretical prediction due to its non-Gaussian nature. In particular, the shape of $p(x,v)$ becomes asymmetric in v and develops non-Gaussian tails. While the prediction (9) cannot account for the non-Gaussianity induced by the interplay of confinement and spatially modulating swim velocity, we remark that its quality near the regions where the particle preferably accumulates is still very good. This conclusion resembles the one obtained in Ref. [91], where an AOUP (with $u(x) = v_0$) has been studied in a single-well anharmonic confinement.

Finally, the large-persistence regime, $v_0\tau/S \gg 1$, where the density distribution has multiple peaks also gives rise to a rich phenomenology of the stationary velocity profile, as shown in Fig. 3 (g) and (h). In the spatial regions for which $\Lambda(x) > 0$, i.e., where the particles accumulate, the velocity distribution $p(x,v)$ (at fixed x) is again well described by the Gaussian distribution with position-dependent variance given by Eq. (9) (see Fig. 3 (g)), as in the case $v_0\tau/S \lesssim 1$. Instead, in the spatial regions where $\Lambda(x) < 0$, i.e., between the primary and the secondary peaks (see also Fig. 2 (c)), the distribution displays a non-Gaussian shape (see Fig. 3 (h)). Compared to the case $v_0\tau/S \sim 1$, the non-Gaussianity is much more evident due to the occurrence of a bimodal behavior in the velocity distribution. In more detail, upon shifting the coordinate x in the first argument of $p(x,v)$ closer to the origin (Fig. 3 (g) and (h)), we observe that, starting from a nearly Gaussian shape centered at $v = 0$ (pink curve), the main peak moves toward $v < 0$ and a second small peak starts growing for $v > 0$ (brown curve). Shifting again x, the second peak becomes dominant (yellow curve) and moves closer toward $v = 0$ until the distribution is again described by a Gaussian (green curve). This phenomenology resembles the one observed in the case of an AOUP with $u(x) = v_0$ in a double-well potential [96]. Also in the latter case, the velocity distribution at fixed position exhibits bimodality in the spatial regions where the effective friction coefficient $\Lambda(x) \simeq \Gamma(x)$ becomes negative, although this effect is then induced by the negative curvature of the potential. Intuitively, particles that are stuck in an accumulation region placed far from the potential minima (where $u(x)\eta$ balances the confining force) could move back towards the center or other minima when their active force varies because of the noise fluctuations. For example, when η changes sign (or $|\eta|$ decreases), the particle comes back leftward or rightward (depending on the sign of η) moving with a large velocity induced by the deterministic force (that is particularly large far from the potential minimum) until to reach a new accumulation region. This simple argument provides an additional intuitive explanation for the bimodality of the velocity distribution.

4.4 Spatial profile of the kinetic temperature

To emphasize the dynamical effects due to the spatial modulation of the swim velocity, we focus on the profile of the kinetic temperature defined as the variance of the particle velocity, $\langle v^2(x)\rangle$. We show $\langle v^2(x)\rangle$ as a function of x in Fig. 4 for values of $v_0\tau/S$ spanning all regimes from small (panel (c)) to intermediate and large persistence (panel (d)), see also panels (a) and (b) for a direct comparison with the corresponding density profiles.

For small values of $v_0\tau/S \ll 1$, the spatial profile of the variance, $\langle v^2(x)\rangle$, is rather flat and attains its maximum value at $x = 0$, i.e., the position of the potential minimum (see Fig. 4 (c)). When $v_0\tau/S$ increases, e.g., due to a shorter periodicity S of the swim-velocity $u(x)$, $\langle v^2(x)\rangle$ decreases upon moving away from the potential minimum. This is consistent with the scenario observed in Fig. 4 (a): the particles accumulate in the regions where they move slowly and the velocity variance is small. Such a result agrees with the observed behavior in the potential-free case (such that $u(x)$ coincides the particle velocity), where the particles accumulate in regions corresponding to the minima of $u(x)$, according to the law $\rho(x) \sim 1/u(x)$. In this regime, the

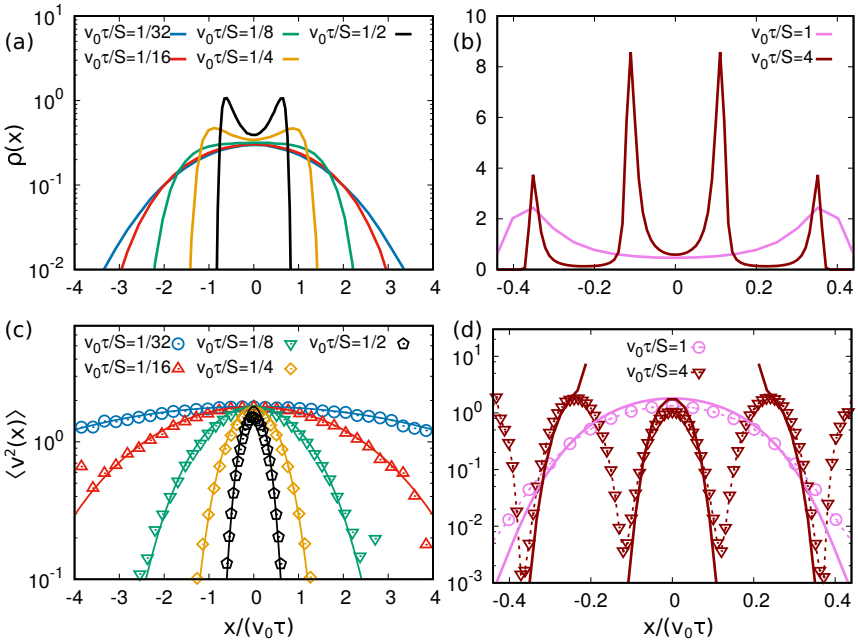

Figure 4: Spatial profile of the kinetic temperature. Panels (a) and (b): simulated density profile $\rho(x)$ for different values of the dimensionless parameter $v_0\tau/S$ as a reference. Panels (c) and (d): kinetic temperature $\langle v^2(x)\rangle$ with the same color legend. In particular, panels (a) and (c) show the small-persistence regime, $v_0\tau/S \leq 1$, while panels (b) and (d) display the intermediate-persistence and large-persistence regimes, namely $v_0\tau/S \sim 1$ and $v_0\tau/S \geq 1$, respectively. Colored symbols (and dotted lines drawn as a guide to the eye) are obtained from numerical simulations while solid colored lines show the theoretical prediction (11) (in the regions where $\Lambda(x)$, given by Eq. (19), is positive definite). Simulations are realized in one spatial dimension with $\tau k/\gamma = 1$ and $\alpha = 0.9$.

comparison between numerical data and the theoretical prediction (11) (with $\Lambda(x)$ given by Eq. (19)) shows a good agreement.

For larger values of $v_0\tau/S$ (large-persistence regime), the velocity variance shows a more complex profile (see Fig. 4 (d)), which resembles the oscillating shape of $u(x)$. In particular, $\langle v^2(x)\rangle$ is very small near the peaks of the density distribution, while it assumes larger values in the regions where the density is very small and the probability of finding a particle is very low. This finding is consistent with the fact that active particles accumulate in the regions where the velocity variance is small and the observation of an increasing number of such regions for increasing $v_0\tau/S$. Finally, in this regime, the prediction (11) reproduces quite well the behavior near the origin but fails further away from it, specifically, in the regions where the effective friction displays negative values, $\Lambda(x) < 0$.

5 Conclusion

In this paper, we have investigated the stationary behavior of an active particle subject to two competing spatially dependent drivings: the self-propulsion velocity and the external force. While the two mechanisms were already investigated separately, to the best of our knowledge, this is the first time that their interplay has been considered. Starting from a Fokker-Planck description of the particle's dynamics in our generalized AOUP model [56], we have developed

a theoretical treatment, which provides the steady-state distribution (9) of both positions and velocities as a function of the input potential and of the swim-velocity profile. The theory presented here contains as special cases both the UCNA describing the time evolution of distribution of positions and velocities of an AOUP with constant swim velocity in an external field [59, 88], and the recent theory of a free AOUP driven by an inhomogeneous propulsion force, which is exact in the stationary case [74]. Our theoretical method is exact in the small-persistence regime, where it is consistent with the results obtained through an exact perturbative method, and also provides a useful approximation to qualitatively predict the shape of the distributions in the large-persistence regime.

Specifically, we have applied our theory to a one-dimensional AOUP in a sinusoidal motility landscape subject to a harmonic potential, such that the deviations of the velocity distributions from a Gaussian shape exclusively arise from the interplay of these two fields. We corroborated all theoretical predictions by numerical simulations and found a good agreement. The system revealed an intriguing scenario determined by the joint action of the self-propulsion velocity gradient and the external force. While, in the regime of small persistence, both the density and the velocity distributions are bell shaped and well-approximated by Gaussians, we predict that, as the persistence length becomes comparable with the spatial period of the swim velocity, a transition from a unimodal to a bimodal density occurs, also accompanied by a strong non-Gaussian effects in the velocity distribution. Interestingly, in the large-persistence regime, as the density shows multi-modality, the velocity distribution becomes bimodal in the spatial regions between two successive peaks of the density.

Despite our particular attention to one spatial dimension, we recall that we practically obtain the same results for a planar geometry in higher spatial dimensions and that we expect that our theory is also suitable for sufficiently well-behaved potentials and velocity fields in other geometries (compare the discussion in Sec. 3.1). While, for active colloids, the emergence of an additional effective torque due to the spatial modulation of the swim velocity could be responsible for an even more complex phenomenology [16, 19], we outline that our theory should be suitable in the case of engineered bacteria whose velocity profile can be manipulated by external light [25, 27]. From a pure theoretical perspective, our techniques may also be extended and applied to more complex dynamics, for instance accounting for the presence of thermal noise [72, 75], a spatially dependent torque [16, 19], or additional competing nonconservative force fields like a Lorentz force [103]. A final challenging research point concerns the dynamical properties of our model and, in particular, the extension of the theory to time-dependent swim-velocity profiles $u(x, t)$, for instance in the form of traveling waves [23, 24, 49].

In conclusion, we have shown that the interplay between an external force and a spatially modulating swim velocity can be used to tune the behavior of a confined active particle, for instance by locally increasing the kinetic temperature or by forcing the particles to accumulate in particular spatial regions with different probability. We demonstrated that by combining these two physically distinct effects, it is possible to generate two complex density patterns through relatively simple fields, which is surely easier to realize in practice than generating a single external field with a complex shape. This possibility to fine-tune the stationary properties of active particles in experimental systems opens up a new avenue for future applications and developments.

Acknowledgements

LC and UMBM warmly thank Andrea Puglisi for letting us use the computer facilities of his group and for discussions regarding some aspects of this research.

5.0.0.1 Funding information LC and UMBM acknowledge support from the MIUR PRIN 2017 project 201798CZLJ. LC acknowledges support from the Alexander Von Humboldt foundation. RW and HL acknowledge support by the Deutsche Forschungsgemeinschaft (DFG) through the SPP 2265, under grant numbers WI 5527/1-1 (RW) and LO 418/25-1 (HL).

A Derivation of the auxiliary dynamics (6)

To derive the auxiliary dynamics (6), we start from Eq. (2a) chosing $D_t = 0$. We recall that following Ref. [75] it is possible to generalize the procedure also to include the more general case with $D_t > 0$. At first, we take the time-derivative of Eq. (2a), obtaining:

$$\gamma\ddot{\mathbf{x}} = -\nabla\nabla U\cdot\dot{\mathbf{x}} + \gamma\boldsymbol{\eta}\left(\frac{\partial}{\partial t} + \mathbf{v}\cdot\nabla\right)u(\mathbf{x},t) + \gamma u(\mathbf{x},t)\dot{\boldsymbol{\eta}}\,. \tag{22}$$

By defining the $\mathbf{v} = \dot{\mathbf{x}}$ as the particle velocity and replacing $\dot{\mathbf{f}}_a$ with the dynamics (2b), we get:

$$\gamma\dot{\mathbf{v}} = -\nabla\nabla U\cdot\mathbf{v} + \gamma\boldsymbol{\eta}\left(\frac{\partial}{\partial t} + \mathbf{v}\cdot\nabla\right)u(\mathbf{x},t) + \gamma u(\mathbf{x},t)\left(-\frac{\boldsymbol{\eta}}{\tau} + \frac{\sqrt{2}}{\sqrt{\tau}}\boldsymbol{\chi}\right). \tag{23}$$

Finally, by replacing $\boldsymbol{\eta}$ in favor of $\mathbf{v}$ and $\mathbf{x}$, taking advantage of the relation (2a), we obtain the dynamics (6).

We remind that this sequence of operation is fully equivalent to performing a change of variables, by considering that the dynamics (2a) is a deterministic relation that allows us to replace $\boldsymbol{\eta}$ with $\mathbf{x}$ and $\mathbf{v}$. The Jacobian matrix $\mathcal{J}$ of this transformation $\mathbf{a} = (\mathbf{x},\boldsymbol{\eta}) \to \mathbf{b} = (\mathbf{x}',\mathbf{v})$ with $\mathbf{x}' = \mathbf{x}$ reads:

$$\mathcal{J} = \frac{\partial\mathbf{b}}{\partial\mathbf{a}} = \begin{bmatrix} \frac{\partial\mathbf{x}'}{\partial\mathbf{x}} & \frac{\partial\mathbf{x}'}{\partial\boldsymbol{\eta}} \\ \frac{\partial\mathbf{v}}{\partial\mathbf{x}} & \frac{\partial\mathbf{v}}{\partial\boldsymbol{\eta}} \end{bmatrix} = \begin{bmatrix} 1 & 0 \\ 0 & u(\mathbf{x}) \end{bmatrix}. \tag{24}$$

The determinant of this matrix, $\det[\mathcal{J}] = u(\mathbf{x})$, yields the Jacobian of the transformation as stated in Eq. (4).

B Derivation of predictions (9) and (10)

To predict the shape of the stationary probability distributions, $p(\mathbf{x},\mathbf{v})$ and $\rho(\mathbf{x})$, stated in Sec. 3, we start from the dynamics in the variables $\mathbf{x}$ and $\mathbf{v}$, namely Eq. (6), for a static profile of the swim velocity, $u(\mathbf{x})$. Switching to the Fokker-Planck equation for $p = p(\mathbf{x},\mathbf{v},t)$, we obtain the exact time evolution:

$$\partial_t p = \nabla_v\cdot\left(\frac{\boldsymbol{\Gamma}}{\tau}\cdot\mathbf{v}p + \frac{u^2(\mathbf{x})}{\tau}\nabla_v p\right) - \mathbf{v}\cdot\nabla p + \nabla\cdot\frac{\nabla U}{\gamma\tau}p - \nabla_v\cdot\frac{[\gamma\mathbf{v}+\nabla U]}{\gamma u(\mathbf{x})}(\mathbf{v}\cdot\nabla)u(\mathbf{x}), \tag{25}$$

where ∇ and ∇_v are the vectorial derivative operators in position and velocity space, respectively. Balancing the diffusion term (proportional to the Laplacian of $\mathbf{v}$) and the other effective friction terms (say the one linearly proportional to $\mathbf{v}$), we get the approximate condition [82]:

$$0 = \nabla_v\cdot\left(\frac{\boldsymbol{\Lambda}}{\tau}\cdot\mathbf{v}p + \frac{u^2(\mathbf{x})}{\tau}\nabla_v p\right) \tag{26}$$

with the effective friction matrix

$$\boldsymbol{\Lambda}(\mathbf{x}) = \mathbf{I} + \frac{\tau}{\gamma}\nabla\nabla U(\mathbf{x}) - \frac{\tau}{\gamma}\nabla U(\mathbf{x})\frac{\nabla u(\mathbf{x})}{u(\mathbf{x})}, \tag{27}$$

that has been defined in Eq. (8). The condition (26) corresponds to requiring that the divergence of the irreversible (with respect to time-reversal transformations) currents is zero. To proceed further, we require that the irreversible currents vanish, i.e., that the expression in the brackets of Eq (26) is zero in the same spirit of Ref. [88]. This choice is consistent with an effective equilibrium approach and allows us to find the explicit approximate steady-state solution for $p(\mathbf{x},\mathbf{v})$ as

$$p(\mathbf{x},\mathbf{v}) \propto g(\mathbf{x}) \exp\left(-\frac{\mathbf{v}\cdot\boldsymbol{\Lambda}(\mathbf{x})\cdot\mathbf{v}}{2u^2(\mathbf{x})}\right), \tag{28}$$

where $g(\mathbf{x})$ is a function purely depending on $\mathbf{x}$, which is still to be determined. Expressing $g(\mathbf{x}) = \rho(\mathbf{x})\sqrt{\det[\boldsymbol{\Lambda}(\mathbf{x})]}/(\sqrt{2\pi}u(\mathbf{x}))$ without loss of generality, we obtain Eq. (9), where $\rho(\mathbf{x})$ represents the density of the system derived below.

To determine the function $\rho(\mathbf{x})$, we first identify the acceleration term [78]

$$u(\mathbf{x})\frac{d}{dt}\frac{\mathbf{v}}{u(\mathbf{x})} = \dot{\mathbf{v}} - \frac{\mathbf{v}}{u(\mathbf{x})}(\mathbf{v}\cdot\nabla)u(\mathbf{x}) \tag{29}$$

in the dynamics (6) with $\partial u(\mathbf{x})/\partial t = 0$. Assuming that the velocity relaxes faster than the position (as for example in the small-persistence regime) allows us to neglect both these terms in Eq. (6), obtaining the following overdamped equation:

$$\dot{\mathbf{x}} = -\frac{1}{\gamma}\boldsymbol{\Lambda}^{-1}\cdot\nabla U + \sqrt{2\tau}u(\mathbf{x})\boldsymbol{\Lambda}^{-1}\cdot\boldsymbol{\chi}\,. \tag{30}$$

From this dynamics, it is convenient to switch to the effective Smoluchowski equation for the density of the system, $\rho(\mathbf{x},t)$, and use the Stratonovich convention, obtaining:

$$\frac{\partial\rho}{\partial t} = \frac{\partial}{\partial x_i}\left(\frac{1}{\gamma}\Lambda^{-1}_{ij}\left(\frac{\partial U}{\partial x_j}\right)\rho + \tau u\Lambda^{-1}_{ik}\frac{\partial}{\partial x_j}\left[\Lambda^{-1}_{jk}u\rho\right]\right). \tag{31}$$

Here and in what follows, we have explicitly written Latin indices for the spatial components of vectors and matrices and adopted also the Einstein's convention for repeated indices, for convenience.

To proceed, we assume the zero-current condition (as in Refs. [59, 104]), obtaining an effective equation for the stationary density $\rho(\mathbf{x})$:

$$\frac{1}{\gamma}\Lambda^{-1}_{ij}\left(\frac{\partial U}{\partial x_j}\right)\rho + \tau u\Lambda^{-1}_{ik}\frac{\partial}{\partial x_j}\left[\Lambda^{-1}_{jk}u\rho\right] = 0\,. \tag{32}$$

Multiplying by $\Lambda_{lh}\Lambda_{hi}$ and summing over repeated indices, we get the following relation after some algebraic manipulations

$$\frac{1}{\gamma\tau u^2}\Lambda_{lj}\frac{\partial U}{\partial x_j} + \Lambda_{lk}\frac{\partial}{\partial x_j}\Lambda^{-1}_{jk} + \frac{\Lambda_{lk}\Lambda^{-1}_{jk}}{u\rho}\frac{\partial}{\partial x_j}[u\rho] = 0\,, \tag{33}$$

whose solution for the density distribution $\rho(\mathbf{x})$ reads:

$$\rho(\mathbf{x}) \approx \frac{\mathcal{N}}{u(\mathbf{x})}\exp\left(\frac{1}{\gamma\tau}\int^{x} d\mathbf{y}\cdot\frac{\boldsymbol{\Lambda}(\mathbf{y})\cdot\mathbf{F}(\mathbf{y})}{u^2(\mathbf{y})} + \int^{x} d\mathbf{y}\cdot\boldsymbol{\Lambda}(\mathbf{y})\cdot\nabla\cdot\boldsymbol{\Lambda}^{-1}(\mathbf{y})\right). \tag{34}$$

Finally, by assuming a planar symmetry for both u and U, we have $\nabla\cdot\boldsymbol{\Lambda}^{-1} \equiv \hat{e}_x\cdot\partial\boldsymbol{\Lambda}^{-1}/\partial x$, where $\hat{e}_x$ denotes the unit vector corresponding to the coordinate x, and can therefore use the explicit Jacobi relation

$$\boldsymbol{\Lambda}\cdot\hat{e}_x\cdot\frac{\partial\boldsymbol{\Lambda}^{-1}}{\partial x} = -\frac{1}{\det[\boldsymbol{\Lambda}]}\hat{e}_x\frac{\partial\det[\boldsymbol{\Lambda}]}{\partial x} = -\hat{e}_x\frac{\partial\ln\det[\boldsymbol{\Lambda}]}{\partial x} \tag{35}$$

for the determinant $\det \mathbf{\Lambda}$ of a matrix $\mathbf{\Lambda}$. We remark that the general relation

$$\mathbf{\Lambda} \cdot \nabla \cdot \mathbf{\Lambda}^{-1} = -\nabla \ln \det[\mathbf{\Lambda}] \tag{36}$$

only holds in the above planar case (35) or for a constant swim velocity $u(\boldsymbol{x}) = v_0$, see also appendix B of Ref. [72]. However, since there are no conceptual differences, we can plug the approximation (36) into the prediction (34) to obtain the compact representation (10) of $\rho(\boldsymbol{x})$ in the main text.

The same stationary condition (33) can be obtained using the Fox approach [81] (when generalized to multiple components [105, 106]), while the corresponding time evolution differs from the UCNA dynamics (31) by the additional occurrence of the factors Λ_{ij}^{-1} and Λ_{ik}^{-1} therein. Note that, if we do not neglect the thermal Brownian noise in Eq. (2), also the stationary predictions of Fox and UCNA differ, even for a spatially constant swim velocity [72].

C Multi-scale technique: derivation of Eq. (14)

In this appendix, we derive the perturbative result (14) for the probability distribution $p(x, v)$ in the one-dimensional active system described by the Fokker-Planck equation (13). We adopt the multiple-time-scale technique, which is designed to deal with problems with fast and slow degrees of freedom. In the regime of small persistence time (where τ is the smallest time scale of the system), the dynamics (13) exhibits the separation of time scales: in this case, the particle velocity rapidly arranges according to its stationary distribution and the spatial distribution evolves on a slower time scale.

To derive the multiple-time expansion, let us introduce the following dimensionless variables:

$$\tilde{t} = t\frac{v_0}{S}, \tag{37}$$

$$X = \frac{x}{S}, \tag{38}$$

$$V = \frac{v}{v_0}, \tag{39}$$

$$\tilde{F}(X) = -\frac{S}{v_0^2 \tau \gamma}\frac{\partial U(x)}{\partial x}, \tag{40}$$

$$\tilde{\Gamma}(X) = 1 - \tau^2 \frac{v_0^2}{S^2}\frac{\partial \tilde{F}(X)}{\partial X}, \tag{41}$$

$$w(X) = \frac{u(x)}{v_0}, \tag{42}$$

and the small expansion parameter $\zeta^{-1} \propto \tau$, where

$$\zeta = \frac{S}{\tau v_0} \tag{43}$$

is the ratio between the spatial period of the swim velocity S and the persistence length of the self-propulsion velocity $v_0\tau$. With our choice, a large (small) value of ζ corresponds to the small-persistence (large-persistence) regime. Now, we express the Fokker-Planck equation (13) in these variables and find:

$$\begin{aligned}&\frac{\partial P(X,V,\tilde{t})}{\partial \tilde{t}} + V\frac{\partial}{\partial X}P + \tilde{F}(X)\frac{\partial}{\partial V}P + \frac{1}{\zeta}R(X)\frac{\partial}{\partial V}VP \\ &+\frac{1}{w(X)}\frac{\partial}{\partial X}w(X)\frac{\partial}{\partial V}(V^2 P) = \zeta L_{\mathrm{FP}} P\,,\end{aligned} \tag{44}$$

where we have further introduced the operator

$$L_{\rm FP} \equiv \frac{\partial}{\partial V}\Big(V + w^2(X)\frac{\partial}{\partial V}\Big) \tag{45}$$

and the function

$$R(X) \equiv \Big[\frac{\partial \tilde{F}}{\partial X} - \tilde{F}(X)\frac{1}{w(X)}\frac{\partial}{\partial X}w(X)\Big], \tag{46}$$

for convenience.

To develop our perturbative solution, we notice that the local operator $L_{\rm FP}$ is proportional to the inverse expansion parameter ζ in Eq. (44). We find that $L_{\rm FP}$ has the following integer eigenvalues:

$$\nu = 0, -1, -2, \ldots \tag{47}$$

and the Hermite polynomials as eigenfunctions:

$$H_\nu(X,V) = \frac{(-1)^\nu}{\sqrt{2\pi}}\,(w(X))^{(\nu-1)}\,\frac{\partial^\nu}{\partial V^\nu}\,e^{-\frac{V^2}{2w^2(X)}}\,. \tag{48}$$

Using these basis functions, we obtain the ansatz to write the solution of the partial differential equation as a linear combination:

$$P(X,V,\tilde{t}) = \sum_{\nu=0}^{\infty}\phi_\nu(X,\tilde{t})H_\nu(X,V)\,. \tag{49}$$

Upon substituting the expansion (49) in Eq. (44) and replacing $L_{\rm FP}$ by its eigenvalues, we obtain the equation:

$$\begin{aligned}
&-\zeta\sum_\nu \nu\,\phi_\nu H_\nu = \sum_\nu \frac{\partial\phi_\nu}{\partial\tilde{t}}H_\nu \\
&+\sum_\nu VH_\nu\frac{\partial}{\partial X}\phi_\nu + \sum_\nu \phi_\nu V\frac{\partial}{\partial X}H_\nu + \tilde{F}\sum_\nu \phi_\nu\frac{\partial}{\partial V}H_\nu \\
&+\frac{w'}{w}\sum_\nu \phi_\nu\frac{\partial}{\partial V}V^2H_\nu + \frac{1}{\zeta}R\sum_\nu\phi_\nu\frac{\partial}{\partial V}VH_\nu\,,
\end{aligned} \tag{50}$$

from which we must determine the unknown functions $\phi_\nu(x,t)$.

Now, instead of truncating arbitrarily the infinite series in Eq. (50) at some order ν, we consider the multiple-time expansion which orders the series in powers of the small parameter $1/\zeta$. In such a way we perform an expansion near the equilibrium solution. To this end, each amplitude ϕ_ν (apart from $\phi_0(X,\tilde{t})$ which is of order ζ^0) is expanded in powers of $1/\zeta$ as:

$$\phi_\nu(X,\tilde{t}) = \sum_{s=0}^{\infty}\frac{1}{\zeta^s}\psi_{s\nu}(X,\tilde{t})\,. \tag{51}$$

Then, we replace the actual probability distribution $P(X,V,\bar{t})$ by an auxiliary distribution $P_{\rm a}(X,V,\bar{t}_0,\bar{t}_1,\bar{t}_2,\ldots)$, which reads:

$$P_{\rm a} = \sum_{s=0}^{\infty}\frac{1}{\zeta^s}\sum_{\nu=0}^{\infty}\psi_{s\nu}(X,\bar{t}_0,\bar{t}_1,\bar{t}_2,\ldots)H_\nu(X,V)\,. \tag{52}$$

This distribution depends on many time variables $\{\bar{t}_s\}$, associated with the perturbation order s, which are defined as $\bar{t}_s = \bar{t}/\zeta^s$. The time derivative with respect to $\bar{t}$ is then expressed as the sum of partial time-like derivatives:

$$\frac{\partial}{\partial\bar{t}} = \frac{\partial}{\partial\bar{t}_0} + \frac{1}{\zeta}\frac{\partial}{\partial\bar{t}_1} + \frac{1}{\zeta^2}\frac{\partial}{\partial\bar{t}_2} + \ldots\,. \tag{53}$$

Substituting the expansions (51) and (53) into Eq. (50) one obtains at each order $1/\zeta^s$ and for each Hermite function an equation involving the amplitudes $\psi_{sv}(X,\tilde{t})$. The perturbative structure of the resulting set of equations is such that the amplitudes $\psi_{sv}(X,\tilde{t})$ can be obtained by the amplitudes of the lower order $(s-1)$. In particular, we find the following equation for $\psi_{00}=\phi_0$

$$\frac{\partial\psi_{00}(X,\tilde{t})}{\partial\tilde{t}} = \frac{1}{\zeta}\frac{\partial}{\partial X}\Big[w(X)\frac{\partial}{\partial X}\Big(w(X)\psi_{00}\Big) \\ -\tilde{F}(X)\psi_{00}+\frac{1}{\zeta^2}w(X)\frac{\partial}{\partial X}\Big(w(X)R\psi_{00}\Big)\Big], \tag{54}$$

whose steady-state solution reads

$$\psi_{00}(X)=\frac{\mathcal{N}}{w(X)}\Big(1-\frac{1}{\zeta^2}R(X)\Big)\times\exp\left[\int^X dy\,\frac{\tilde{F}(y)}{w^2(y)}\Big(1-\frac{1}{\zeta^2}R(y)\Big)\right], \tag{55}$$

where $\mathcal{N}$ is a normalization factor. In our perturbative procedure, all the remaining amplitudes are expressed in terms of the pivot function $\psi_{00}(X)$. The steady-state amplitudes of the higher-order Hermite polynomials are given by:

$$\psi_{22}=\frac{1}{2}R(X)\psi_{00} \tag{56}$$

$$\psi_{33}(X)=-\frac{1}{6}w(X)\psi_{00}(X)\frac{\partial}{\partial X}R(X) \tag{57}$$

$$\psi_{42}=-\frac{3}{2}\frac{\partial}{\partial X}[w(X)\psi_{33}]+R(X)\psi_{22} \tag{58}$$

$$\psi_{44}(X)=-\frac{1}{4}\Big(\frac{\partial}{\partial X}[w(X)\psi_{33}]-R(X)\psi_{22}\Big), \tag{59}$$

where we have reported only the nonvanishing coefficients for $s\leq 4$. Note that, if $v>s$, the coefficients ψ_{sv} are always zero.

Once Eq. (55) and the coefficients of the double series (52) have been determined, one returns to the original dimensional variables and obtains the perturbative result for $p(x,v)$ reported in Eq. (14).

References

[1] C. Bechinger, R. Di Leonardo, H. Löwen, C. Reichhardt, G. Volpe and G. Volpe, *Active particles in complex and crowded environments*, Reviews of Modern Physics **88**(4), 045006 (2016).

[2] M. Marchetti, J. Joanny, S. Ramaswamy, T. Liverpool, J. Prost, M. Rao and R. A. Simha, *Hydrodynamics of soft active matter*, Reviews of Modern Physics **85**, 1143 (2013).

[3] J. Elgeti, R. G. Winkler and G. Gompper, *Physics of microswimmers—single particle motion and collective behavior: a review*, Reports on Progress in Physics **78**(5), 056601 (2015).

[4] G. Gompper, R. G. Winkler, T. Speck, A. Solon, C. Nardini, F. Peruani, H. Löwen, R. Golestanian, U. B. Kaupp, L. Alvarez *et al.*, *The 2020 motile active matter roadmap*, Journal of Physics: Condensed Matter **32**(19), 193001 (2020).

[5] F. A. Lavergne, H. Wendehenne, T. Bäuerle and C. Bechinger, *Group formation and cohesion of active particles with visual perception–dependent motility*, Science **364**(6435), 70 (2019).

[6] A. R. Sprenger, M. A. Fernandez-Rodriguez, L. Alvarez, L. Isa, R. Wittkowski and H. Löwen, *Active brownian motion with orientation-dependent motility: theory and experiments*, Langmuir **36**(25), 7066 (2020).

[7] M. A. Fernandez-Rodriguez, F. Grillo, L. Alvarez, M. Rathlef, I. Buttinoni, G. Volpe and L. Isa, *Feedback-controlled active brownian colloids with space-dependent rotational dynamics*, Nature communications **11**(1), 1 (2020).

[8] M. Fränzl and F. Cichos, *Active particle feedback control with a single-shot detection convolutional neural network*, Scientific reports **10**(1), 1 (2020).

[9] J. M. Walter, D. Greenfield, C. Bustamante and J. Liphardt, *Light-powering escherichia coli with proteorhodopsin*, Proceedings of the National Academy of Sciences **104**(7), 2408 (2007).

[10] I. Buttinoni, G. Volpe, F. Kümmel, G. Volpe and C. Bechinger, *Active brownian motion tunable by light*, Journal of Physics: Condensed Matter **24**(28), 284129 (2012).

[11] J. Palacci, S. Sacanna, A. P. Steinberg, D. J. Pine and P. M. Chaikin, *Living crystals of light-activated colloidal surfers*, Science **339**(6122), 936 (2013).

[12] B. Dai, J. Wang, Z. Xiong, X. Zhan, W. Dai, C.-C. Li, S.-P. Feng and J. Tang, *Programmable artificial phototactic microswimmer*, Nature Nanotechnology **11**(12), 1087 (2016).

[13] W. Li, X. Wu, H. Qin, Z. Zhao and H. Liu, *Light-driven and light-guided microswimmers*, Advanced Functional Materials **26**(18), 3164 (2016).

[14] W. Uspal, *Theory of light-activated catalytic janus particles*, The Journal of Chemical Physics **150**(11), 114903 (2019).

[15] A. P. Bregulla, H. Yang and F. Cichos, *Stochastic localization of microswimmers by photon nudging*, Acs Nano **8**(7), 6542 (2014).

[16] S. Jahanshahi, C. Lozano, B. Liebchen, H. Löwen and C. Bechinger, *Realization of a motility-trap for active particles*, Communications Physics **3**(1), 1 (2020).

[17] N. A. Söker, S. Auschra, V. Holubec, K. Kroy and F. Cichos, *How activity landscapes polarize microswimmers without alignment forces*, Physical Review Letters **126**(22), 228001 (2021).

[18] S. Auschra and V. Holubec, *Density and polarization of active brownian particles in curved activity landscapes*, Physical Review E **103**(6), 062604 (2021).

[19] C. Lozano, B. Ten Hagen, H. Löwen and C. Bechinger, *Phototaxis of synthetic microswimmers in optical landscapes*, Nature Communications **7**, 12828 (2016).

[20] C. Maggi, F. Saglimbeni, M. Dipalo, F. De Angelis and R. Di Leonardo, *Micromotors with asymmetric shape that efficiently convert light into work by thermocapillary effects*, Nature Communications **6**, 7855 (2015).

[21] G. Vizsnyiczai, G. Frangipane, C. Maggi, F. Saglimbeni, S. Bianchi and R. Di Leonardo, *Light controlled 3d micromotors powered by bacteria*, Nature Communications **8**, 15974 (2017).

[22] J. Stenhammar, R. Wittkowski, D. Marenduzzo and M. E. Cates, *Light-induced self-assembly of active rectification devices*, Science Advances **2**(4), e1501850 (2016).

[23] N. Koumakis, A. T. Brown, J. Arlt, S. E. Griffiths, V. A. Martinez and W. C. Poon, *Dynamic optical rectification and delivery of active particles*, Soft Matter **15**(35), 7026 (2019).

[24] C. Lozano, B. Liebchen, B. Ten Hagen, C. Bechinger and H. Löwen, *Propagating density spikes in light-powered motility-ratchets*, Soft Matter **15**(26), 5185 (2019).

[25] J. Arlt, V. A. Martinez, A. Dawson, T. Pilizota and W. C. K. Poon, *Painting with light-powered bacteria*, Nature Communications **9**, 768 (2018).

[26] J. Arlt, V. A. Martinez, A. Dawson, T. Pilizota and W. C. Poon, *Dynamics-dependent density distribution in active suspensions*, Nature Communications **10**, 2321 (2019).

[27] G. Frangipane, D. Dell'Arciprete, S. Petracchini, C. Maggi, F. Saglimbeni, S. Bianchi, G. Vizsnyiczai, M. L. Bernardini and R. Di Leonardo, *Dynamic density shaping of photokinetic e. coli*, Elife **7**, e36608 (2018).

[28] M. J. Schnitzer, *Theory of continuum random walks and application to chemotaxis*, Physical Review E **48**(4), 2553 (1993).

[29] J. Tailleur and M. Cates, *Statistical mechanics of interacting run-and-tumble bacteria*, Physical Review Letters **100**(21), 218103 (2008).

[30] A. Sharma and J. M. Brader, *Brownian systems with spatially inhomogeneous activity*, Physical Review E **96**(3), 032604 (2017).

[31] P. K. Ghosh, Y. Li, F. Marchesoni and F. Nori, *Pseudochemotactic drifts of artificial microswimmers*, Physical Review E **92**(1), 012114 (2015).

[32] B. Liebchen and H. Löwen, *Optimal navigation strategies for active particles*, EPL (Europhysics Letters) **127**(3), 34003 (2019).

[33] A. Fischer, F. Schmid and T. Speck, *Quorum-sensing active particles with discontinuous motility*, Physical Review E **101**(1), 012601 (2020).

[34] T. Bäuerle, A. Fischer, T. Speck and C. Bechinger, *Self-organization of active particles by quorum sensing rules*, Nature Communications **9**, 3232 (2018).

[35] F. Jose, S. K. Anand and S. P. Singh, *Phase separation of an active colloidal suspension via quorum-sensing*, Soft Matter **17**(11), 3153 (2021).

[36] S. Azimi, A. D. Klementiev, M. Whiteley and S. P. Diggle, *Bacterial quorum sensing during infection*, Annual Review of Microbiology **74**, 201 (2020).

[37] H. D. Vuijk, A. Sharma, D. Mondal, J.-U. Sommer and H. Merlitz, *Pseudochemotaxis in inhomogeneous active brownian systems*, Physical Review E **97**, 042612 (2018).

[38] H. Merlitz, H. D. Vuijk, R. Wittmann, A. Sharma and J.-U. Sommer, *Pseudo-chemotaxis of active brownian particles competing for food*, PLOS ONE **15**(4), 1 (2020).

[39] I. Richard Lapidus, *"pseudochemotaxis" by micro-organisms in an attractant gradient*, Journal of Theoretical Biology **86**(1), 91 (1980).

[40] H. D. Vuijk, H. Merlitz, M. Lang, A. Sharma and J.-U. Sommer, *Chemotaxis of cargo-carrying self-propelled particles*, Physical Review Letter **126**, 208102 (2021).

[41] J. Grauer, H. Löwen and L. M. Janssen, *Spontaneous membrane formation and self-encapsulation of active rods in an inhomogeneous motility field*, Physical Review E **97**(2), 022608 (2018).

[42] M. P. Magiera and L. Brendel, *Trapping of interacting propelled colloidal particles in inhomogeneous media*, Physical Review E **92**(1), 012304 (2015).

[43] C. Maggi, L. Angelani, G. Frangipane and R. Di Leonardo, *Currents and flux-inversion in photokinetic active particles*, Soft Matter **14**(24), 4958 (2018).

[44] H. Merlitz, H. D. Vuijk, J. Brader, A. Sharma and J.-U. Sommer, *Linear response approach to active brownian particles in time-varying activity fields*, The Journal of Chemical Physics **148**(19), 194116 (2018).

[45] C. Lozano and C. Bechinger, *Diffusing wave paradox of phototactic particles in traveling light pulses*, Nature Communications **10**, 2495 (2019).

[46] A. Geiseler, P. Hänggi and F. Marchesoni, *Taxis of artificial swimmers in a spatio-temporally modulated activation medium*, Entropy **19**(3), 97 (2017).

[47] A. Zampetaki, P. Schmelcher, H. Löwen and B. Liebchen, *Taming polar active matter with moving substrates: directed transport and counterpropagating macrobands*, New Journal of Physics **21**(1), 013023 (2019).

[48] W.-j. Zhu, X.-q. Huang and B.-q. Ai, *Transport of underdamped self-propelled particles in active density waves*, Journal of Physics A: Mathematical and Theoretical **51**(11), 115101 (2018).

[49] A. Geiseler, P. Hänggi and F. Marchesoni, *Self-polarizing microswimmers in active density waves*, Scientific Reports **7**, 41884 (2017).

[50] T. Speck, A. M. Menzel, J. Bialké and H. Löwen, *Dynamical mean-field theory and weakly non-linear analysis for the phase separation of active brownian particles*, The Journal of chemical physics **142**(22), 224109 (2015).

[51] M. E. Cates and J. Tailleur, *Motility-induced phase separation*, Annual Review of Condensed Matter Physics **6**(1), 219 (2015).

[52] A. Baskaran and M. C. Marchetti, *Statistical mechanics and hydrodynamics of bacterial suspensions*, Proceedings of the National Academy of Sciences **106**(37), 15567 (2009).

[53] A. P. Solon, J. Stenhammar, R. Wittkowski, M. Kardar, Y. Kafri, M. E. Cates and J. Tailleur, *Pressure and phase equilibria in interacting active brownian spheres*, Physical Review Letters **114**(19), 198301 (2015).

[54] E. Flenner, G. Szamel and L. Berthier, *The nonequilibrium glassy dynamics of self-propelled particles*, Soft matter **12**(34), 7136 (2016).

[55] I. Petrelli, P. Digregorio, L. F. Cugliandolo, G. Gonnella and A. Suma, *Active dumbbells: Dynamics and morphology in the coexisting region*, The European Physical Journal E **41**(10), 128 (2018).

[56] L. Caprini and U. M. B. Marconi, *Spatial velocity correlations in inertial systems of active brownian particles*, Soft Matter **17**(15), 4109 (2021).

[57] G. Negro, C. B. Caporusso, P. Digregorio, G. Gonnella, A. Lamura and A. Suma, *Inertial and hydrodynamic effects on the liquid-hexatic transition of active colloids*, arXiv preprint arXiv:2201.10019 (2022).

[58] E. Chacon, F. Alarcón, J. Ramirez, P. Tarazona and C. Valeriani, *Intrinsic structure perspective for mips interfaces in two dimensional systems of active brownian particles*, Soft Matter (2022).

[59] C. Maggi, U. M. B. Marconi, N. Gnan and R. Di Leonardo, *Multidimensional stationary probability distribution for interacting active particles*, Scientific Reports **5**, 10742 (2015).

[60] G. Szamel, *Self-propelled particle in an external potential: Existence of an effective temperature*, Physical Review E **90**(1), 012111 (2014).

[61] L. Dabelow, S. Bo and R. Eichhorn, *Irreversibility in active matter systems: Fluctuation theorem and mutual information*, Physical Review X **9**(2), 021009 (2019).

[62] L. Berthier, E. Flenner and G. Szamel, *Glassy dynamics in dense systems of active particles*, The Journal of Chemical Physics **150**(20), 200901 (2019).

[63] D. Martin, J. O'Byrne, M. E. Cates, É. Fodor, C. Nardini, J. Tailleur and F. van Wijland, *Statistical mechanics of active ornstein-uhlenbeck particles*, Physical Review E **103**(3), 032607 (2021).

[64] L. Caprini and U. Marini Bettolo Marconi, *Inertial self-propelled particles*, The Journal of Chemical Physics **154**(2), 024902 (2021).

[65] G. H. P. Nguyen, R. Wittmann and H. Löwen, *Active ornstein-uhlenbeck model for self-propelled particles with inertia*, Journal of Physics: Condensed Matter **34**, 035101 (2021).

[66] L. Caprini, A. R. Sprenger, H. Löwen and R. Wittmann, *The parental active model: A unifying stochastic description of self-propulsion*, The Journal of Chemical Physics **156**, 071102 (2022).

[67] Y. Fily and M. C. Marchetti, *Athermal phase separation of self-propelled particles with no alignment*, Physical Review Letter **108**(23), 235702 (2012).

[68] T. F. Farage, P. Krinninger and J. M. Brader, *Effective interactions in active brownian suspensions*, Physical Review E **91**(4), 042310 (2015).

[69] L. Caprini, E. Hernández-García, C. López and U. M. B. Marconi, *A comparative study between two models of active cluster crystals*, Scientific Reports **9**, 16687 (2019).

[70] C. Maggi, M. Paoluzzi, L. Angelani and R. Di Leonardo, *Memory-less response and violation of the fluctuation-dissipation theorem in colloids suspended in an active bath*, Scientific Reports **7**, 17588 (2017).

[71] C. Maes, *Fluctuating motion in an active environment*, Physical Review Letters **125**(20), 208001 (2020).

[72] R. Wittmann, C. Maggi, A. Sharma, A. Scacchi, J. M. Brader and U. M. B. Marconi, *Effective equilibrium states in the colored-noise model for active matter I. pairwise forces in the fox and unified colored noise approximations*, Journal of Statistical Mechanics: Theory and Experiment **2017**(11), 113207 (2017).

[73] The common mapping between ABPs and AOUPs in $d > 1$ spatial dimensions relates the persistence time $\tau = D_r^{-1}/(d-1)$ and the active diffusion coefficient $D_a = v_0^2\tau/d$ of the AOUP model to the rotational diffusivity D_r and self-propulsion-velocity scale v_0 of the ABP model [72]. To ease the notation for the predictions of our generalized AOUP model, we follow the convention of Ref. [74] and do not imply this mapping, simply setting $d = 1$, which gives the same physics. If one wishes to make explicit contact to the ABP model for $d > 1$, the last term in Eq. (2b) should be replaced by $\sqrt{2\tau/d}\boldsymbol{\chi}$, such that the variance of the Ornstein-Uhlenbeck process at equal time becomes unity. Hence, the formulas subsequently derived for arbitrary spatial dimension d should be interpreted by rescaling $u(\mathbf{x}) \to u(\mathbf{x})/\sqrt{d}$.

[74] L. Caprini, U. M. B. Marconi, R. Wittmann and H. Löwen, *Dynamics of active particles with space-dependent swim velocity*, Soft Matter **18**, 1412 (2022).

[75] L. Caprini and U. M. B. Marconi, *Active particles under confinement and effective force generation among surfaces*, Soft Matter **14**(44), 9044 (2018).

[76] To shed light on the essential physical difference between a confined particle with uniform swim velocity and a free particle subject to a swim-velocity profile, let us consider, as a basic example, an AOUP with constant swim velocity $u(\mathbf{x}) = v_0$ trapped in a harmonic potential, system (i), whose exact stationary density profile $\rho(\mathbf{x})$ has a Gaussian shape. In principle, this distribution can also be realized in the absence of external forces by a swim-velocity profile of the form $u(\mathbf{x}) \propto 1/\rho(\mathbf{x})$, system (ii), but the physics are crucially distinct. In case (i), the particle is confined and can explore the region far from the minimum of the potential only because of fluctuations induced by the active force. The Gaussian density profile in system (ii) is obtained because the particle spends more time in the central region where it moves slowly. However, due to the absence of external forces (or other confining mechanisms), the diverging swim velocity allows the particle to escape to infinity. This means that such an effective confinement can only formally be achieved through periodic boundary conditions: the particle moves slowly in the minimum of $u(\mathbf{x})$, escapes rightwards (or leftwards) with an increasing swim velocity and approaches again the slow region by coming back from the other side of the box .

[77] P. Jung and P. Hänggi, *Dynamical systems: a unified colored-noise approximation*, Physical Review A **35**(10), 4464 (1987).

[78] P. Jung and P. Hänggi, *Optical instabilities: new theories for colored-noise-driven laser instabilities*, J. Opt. Soc. Am. B **5**(5), 979 (1988).

[79] P. Hänggi and P. Jung, *Colored noise in dynamical systems*, Advances in Chemical Physics **89**, 239 (1995).

[80] R. F. Fox, *Functional-calculus approach to stochastic differential equations*, Physical Review A **33**, 467 (1986).

[81] R. F. Fox, *Uniform convergence to an effective fokker-planck equation for weakly colored noise*, Phys. Rev. A **34**, 4525 (1986).

[82] U. M. B. Marconi, N. Gnan, M. Paoluzzi, C. Maggi and R. Di Leonardo, *Velocity distribution in active particles systems*, Scientific Reports **6**, 23297 (2016).

[83] L. Caprini and U. Marini Bettolo Marconi, *Active matter at high density: Velocity distribution and kinetic temperature*, The Journal of Chemical Physics **153**(18), 184901 (2020).

[84] L. Bocquet, *High friction limit of the kramers equation: The multiple time-scale approach*, American Journal of Physics **65**(2), 140 (1997).

[85] U. Marini-Bettolo-Marconi, P. Tarazona and F. Cecconi, *Theory of thermostatted inhomogeneous granular fluids: A self-consistent density functional description*, The Journal of chemical physics **126**(16), 164904 (2007).

[86] U. M. Titulaer, *A systematic solution procedure for the fokker-planck equation of a brownian particle in the high-friction case*, Physica A: Statistical Mechanics and its Applications **91**(3-4), 321 (1978).

[87] É. Fodor, C. Nardini, M. E. Cates, J. Tailleur, P. Visco and F. van Wijland, *How far from equilibrium is active matter?*, Physical Review Letters **117**(3), 038103 (2016).

[88] U. M. B. Marconi, A. Puglisi and C. Maggi, *Heat, temperature and clausius inequality in a model for active brownian particles*, Scientific Reports **7**, 46496 (2017).

[89] D. Martin and T. A. de Pirey, *Aoup in the presence of brownian noise: a perturbative approach*, Journal of Statistical Mechanics: Theory and Experiment **2021**(4), 043205 (2021).

[90] Notice the slightly different role of the expansion parameter τ in Eq. (14) for our version of the AOUP model (2), in which we have eliminated the active diffusion coefficient $D_a \propto \tau$ in favor of an expression containing the explicit factor τ .

[91] L. Caprini, U. M. B. Marconi and A. Puglisi, *Activity induced delocalization and freezing in self-propelled systems*, Scientific Reports **9**, 1386 (2019).

[92] D. Breoni, R. Blossey and H. Löwen, *Brownian particles driven by spatially periodic noise*, Eur. Phys. J. E **45** (2022).

[93] S. Das, G. Gompper and R. G. Winkler, *Confined active brownian particles: theoretical description of propulsion-induced accumulation*, New Journal of Physics **20**(1), 015001 (2018).

[94] L. Caprini, A. Puglisi and A. Sarracino, *Fluctuation–dissipation relations in active matter systems*, Symmetry **13**(1), 81 (2021).

[95] L. Dabelow, S. Bo and R. Eichhorn, *How irreversible are steady-state trajectories of a trapped active particle?*, Journal of Statistical Mechanics: Theory and Experiment **2021**(3), 033216 (2021).

[96] L. Caprini, U. Marini Bettolo Marconi, A. Puglisi and A. Vulpiani, *Active escape dynamics: The effect of persistence on barrier crossing*, The Journal of Chemical Physics **150**, 024902 (2019).

[97] F. J. Schwarzendahl and H. Löwen, *Anomalous cooling and overcooling of active systems*, arXiv preprint arXiv:2111.06109 (2021).

[98] L. Caprini, F. Cecconi and U. Marini Bettolo Marconi, *Correlated escape of active particles across a potential barrier*, The Journal of Chemical Physics **155**(23), 234902 (2021).

[99] E. Woillez, Y. Zhao, Y. Kafri, V. Lecomte and J. Tailleur, *Activated escape of a self-propelled particle from a metastable state*, Physical review letters **122**(25), 258001 (2019).

[100] Y. Fily, *Self-propelled particle in a nonconvex external potential: Persistent limit in one dimension*, The Journal of Chemical Physics **150**(17), 174906 (2019).

[101] E. Woillez, Y. Kafri and N. S. Gov, *Active trap model*, Physical Review Letters **124**(11), 118002 (2020).

[102] E. Woillez, Y. Kafri and V. Lecomte, *Nonlocal stationary probability distributions and escape rates for an active ornstein–uhlenbeck particle*, Journal of Statistical Mechanics: Theory and Experiment **2020**(6), 063204 (2020).

[103] H. D. Vuijk, J.-U. Sommer, H. Merlitz, J. M. Brader and A. Sharma, *Lorentz forces induce inhomogeneity and flux in active systems*, Physical Review Research **2**(1), 013320 (2020).

[104] U. M. B. Marconi, M. Paoluzzi and C. Maggi, *Effective potential method for active particles*, Molecular Physics **114**(16-17), 2400 (2016).

[105] M. Rein and T. Speck, *Applicability of effective pair potentials for active brownian particles*, The European Physical Journal E **39**, 84 (2016).

[106] A. Sharma, R. Wittmann and J. M. Brader, *Escape rate of active particles in the effective equilibrium approach*, Physical Review E **95**, 012115 (2017).